Published in final edited form as:
Pain. 2013 November ; 154(11): . doi:10.1016/j.pain.2013.05.033.

Systemic morphine treatment induces changes in firing patterns and responses of nociceptive afferent fibers in mouse glabrous skin

Dale Hogan[1], **Alyssa L. Baker**[1], **Jose A. Morón**[2], and **Susan M. Carlton**[1]

[1]Dept. Neuroscience and Cell Biology, University of Texas Medical Branch, Galveston TX

[2]Dept. Anesthesiology, Columbia University, New York, NY

Abstract

Patients receiving opioids for pain may experience decreased effectiveness of the drug and even abnormal pain sensitivity – either hyperalgesia and/or allodynia. We hypothesize that peripheral nociceptor hyperexcitability contributes to opioid-induced hyperalgesia and test this using an *in vitro* mouse glabrous skin-nerve preparation. Mice were injected i.p. with escalating doses of morphine (5, 8, 10, 15 mg/kg) or saline every 12 h for 48 h and sacrificed ~12 h following the last injection. Receptive fields of nociceptors were tested for mechanical, heat, and cold sensitivity. Activity was also measured during an initial 2 min period and during 5 min periods between stimuli. Aberrant activity was common in fibers from morphine-treated mice but rare in salinetreated mice. Resting background activity was elevated in C-fibers from morphinetreated mice. Both C- and Aδ -fibers had afterdischarge in response to mechanical, heat and/or cold stimulation of the skin as well as spontaneous, unevoked activity. Compared to saline, morphine treatment increased the proportion of fibers displaying polymodal rather than mechanical-only responses. A significant increase in Aδ-mechanoreceptive fibers responding to cold accounted for most of this change. In agreement with this, morphine-treated mice showed increased sensitivity in the cold tail flick test. In morphine-treated mice, aberrant activity and hyperexcitability of nociceptors could contribute to increased pain sensitivity. Importantly, this activity is likely driving central sensitization, a phenomenon contributing to abnormal sensory processing and chronic pain. If similar changes occur in human patients, aberrant nociceptor activity is likely to be interpreted as pain, and could contribute to opioid-induced hyperalgesia.

1. Introduction

Patients receiving opioids for pain management may experience abnormal pain sensitivity – either hyperalgesia (increased pain from a stimulus that normally provokes pain) and/or allodynia (pain due to a stimulus that does not normally provoke pain) [72]. Opioid-induced hyperalgesia (OIH) is defined in animal studies as a decrease of pain threshold from baseline after chronic administration of opioids. OIH has been reported in animal studies over the last three decades [4]. For many years, the clinical community perceived OIH as a phenomenon

[1]To Whom Correspondence Should Be Sent: Dr. Susan M. Carlton, Department of Neuroscience and Cell Biology, University of Texas Medical Branch, Galveston, TX 77555-1069, Phone: (409)772-1703, Fax : (409)762-9382, smcarlto@utmb.edu.

None of the authors had a conflict of interest concerning this work.

of preclinical research and not relevant to the clinic [82]. In recent years, OIH has been recognized as a real syndrome needing to be addressed in humans, though there is still no well accepted definition of OIH in the clinic [82]. It is commonly identified by the decreased analgesic effect of opioid drugs, or a rebound increase in pain sensitivity that develops over a course of opioid treatment [4]. However, hyperalgesia also occurs with the development of tolerance to opioids and as part of the withdrawal syndrome, and thus clinical OIH in the absence of either tolerance or withdrawal has been difficult to establish. Increased pain over the course of opioid treatment in the absence of withdrawal could likely reflect either the development of tolerance (a desensitization process) or an elevation of pronociception (a sensitization process), among other possibilities [7]. In a clinical setting, tolerance can be treated by increasing the opioid dosage, thus reinstating pain relief. By contrast, if a patient is experiencing OIH, increasing the opioid dose may worsen the patient's condition by increasing sensitivity to pain. In addition, increasing the opioid dose without concomitant pain relief can escalate physical dependence and increase the probability of abuse [27]. Thus, OIH is an important clinical issue; however, its underlying mechanisms are poorly understood.

Several molecular mechanisms have been proposed to explain the development of OIH and sensitization including: 1) sensitization of primary afferent neurons, 2) enhanced production and release of excitatory neurotransmitters or suppressed reuptake of these transmitters, 3) sensitization of second-order neurons, 4) neuroplastic changes in the rostroventral medulla [20]. The contribution of primary afferent neurons is arguably the least studied mechanism of OIH. A peripheral contribution is likely given that small diameter cutaneous primary afferents innervating the rat paw express opioid receptors [21,78] and contain opioid peptides [14]. Furthermore, a peripheral, antinociceptive action of opioids has been confirmed in several studies. Peripherally applied opioid receptor agonists induce analgesia [51,52], inhibit hyperalgesia [45], and decrease spontaneous activity of afferent fibers in inflamed tissue [70,86] (however, see [54]). These peripheral effects are thought to be mediated by opioid receptors on the nociceptors and can be eliminated by systemic antagonist treatment. Systemic opioid actions can be blocked by peripherally acting antagonists, further supporting a peripheral anti-nociceptive opioid action [81]. In contrast, we hypothesize that aberrant signaling in nociceptors following high opioid dosing contributes to OIH and test this hypothesis using an *in vitro* skin-nerve preparation and an *in vivo* behavioral assay in opioid-treated mice.

2. Methods

2.1. Animals and morphine treatment

All experiments were approved by the University Animal Care and Use Committee and met the guidelines of both the National Institutes of Health's Guide for the Care and Use of the Laboratory animals (Department of Health, Education, & Welfare publication no. 85-23, revised 1985, USA) and the International Association for the Study of Pain (IASP) [95]. Steps were taken to reduce the number and any unnecessary discomfort of the animals. Male wild-type C57BL6 mice (6–12 wk) from either Jackson Laboratories (Bar Harbor, ME) or Harlan Laboratories (Houston, TX) were housed in the University of Texas Medical Branch (UTMB) Animal Resource Center in a standard animal room with food and water *ad libitum* under controlled conditions of humidity and temperature (21 ± 2°C) and maintained on a 12 h light/dark cycle. Fifty-six mice were used in electrophysiology experiments and 20 were used in behavioral testing. Morphine sulfate from the UTMB hospital pharmacy was dissolved in 0.9% isotonic saline at 1 mg/ml. Mice received four escalating doses of morphine (5, 8, 10, and 15 mg/kg, intraperitoneal) or the same volume of saline, administered at 12 h intervals as previously described [61]. Twelve hours after the last injection, mice were sacrificed by CO_2 inhalation.

2.2. Skin-nerve preparation

The *in vitro* glabrous skin-nerve preparation used was a modification of the rat glabrous skin-nerve prep used in our lab [34]. The glabrous skin from the ankle to the tips of the toes was dissected from the hindpaw leaving a border of hairy skin along each margin. The tibial nerve with the medial and lateral plantar branches (~3 cm free length) was dissected free from the ankle joint and kept intact with the glabrous skin (Fig. 1). All muscle and tendon tissue was carefully removed from the preparation under a dissecting microscope. The preparation was placed corium side up in an organ bath and superfused at 15 ml/min, 32 °C, with an oxygen-saturated, modified synthetic interstitial fluid solution (SIF, in mM: NaCl, 123; KCl, 3.5; MgSO4, 0.7; CaCl2, 2.0; Na gluconate, 9.5; NaH2PO4, 1.7; glucose, 5.5; sucrose, 7.5; and HEPES, 10; pH 7.4 ± 0.05). The plantar nerves were moved into a separate chamber containing a superficial layer of mineral oil and a bottom layer of SIF. On a mirrored stage, the nerves were desheathed and teased apart under a dissecting microscope. Small filaments from either the medial or the lateral plantar nerve were repeatedly split with sharpened watchmaker forceps to obtain the smallest possible nerve bundle without breakage.

2.3. Neurophysiological recording

Neural activity was recorded using gold wire electrodes and a DAM80 differential amplifier (World Precision Instruments, Sarasota, FL). Action potentials were acquired and later analyzed offline on a PC computer-controlled CED1401 interface and Spike2 spike sorting software (CED Ltd., Cambridge, UK). Mechanically-sensitive fibers were identified initially by probing the skin flap with a blunt glass rod. Only units responding to this noxious stimulus were studied in detail. Nociceptors were further defined as highthreshold, slowly adapting mechanoreceptors with a conduction velocity (CV) between 0.2 and 10 m/s. Non-nociceptors were not studied. The CV of each unit was determined by monopolar electrical stimulation (0.3 – 3.0 ms duration, 0.02 – 1.0 mA, train frequency 1 Hz) at the most mechanosensitive site in the receptive field of each unit using a Teflon-coated steel electrode with an uninsulated tip (2 MΩ) that was gently lowered into the receptive field. The CV was determined from the latency of the action potential and the distance from the stimulation electrode to the recording site (measured to the closest millimeter). The mean background rate for each fiber population (Aδ and C) was determined by recording unit activity for 2 min immediately after a newly teased filament was placed on the recording electrode [34].

2.4. Analysis of aberrant activity

Aberrant activity was defined as a period of activity occurring in the absence of heat, cold or mechanical stimulation. Aberrant activity events were defined as a group consisting of at least 20 spikes that lasted at least 5 s and had interspike intervals less than 5 s [11]. These events were categorized as either afterdischarge or spontaneous activity (SA). Afterdischarge was defined as prolonged activity occurring either immediately after or within 30 s of the end of a stimulus. SA occurred either before any stimulation of the unit or began more than 30 s after the end of a stimulus and was thus considered unrelated to the stimulation. Patterns of firing during afterdischarge and SA were further classified as either regular, irregular or bursting based on the variability of interspike intervals. Irregular firing patterns contained highly variable interspike intervals. Regular firing patterns were identified from histograms of interspike intervals that were tightly grouped around the average interspike interval and had a coefficient of variance (mean/standard deviation) of the interspike interval of < 0.6. Burst events were analyzed using the “bursts” script in Spike2. Bursts were defined by an initial interspike interval of less than 80 ms [37,42]. Offset of the burst occurred when the interspike interval was greater than 200 ms. Periods of aberrant activity with at least 40% of the total number of spikes occurring within bursts were categorized as bursting.

2.5. Heat stimulation

After 2 min baseline recording, radiant heat was applied to the receptive field of each unit (Figs. 1, 2A). The heat lamp (made in house) was placed beneath the recording chamber and a temperature probe was placed on the epidermal side of the skin in the receptive field. The light beam was focused through the translucent bottom of the chamber onto the epidermal surface of the skin. A 10 s heat ramp was applied to each unit, starting from the bath temperature of 32 °C and rising to 52 °C on the epidermal side (equivalent to 51 °C on the corium side). A unit was considered heat sensitive if the discharge rate evoked by the heat stimulation was greater than the background mean frequency of that unit measured 10 s immediately preceding the heat stimulus (calculated by the Spike2 “Mean Frequency” function). The temperature at which the first spike was elicited by the heat stimulus was defined as heat threshold if there was no background activity. Units from MOR mice tended to have more background firing; thus, the temperature at which the unit firing frequency exceeded its background mean firing frequency was considered threshold. A 5 min recovery period was allowed after this and all other stimulations to avoid sensitization of the units.

2.6. Cold stimulation

A small plastic hollow well was constructed from a 3 ml plastic syringe. The luer connector was cut off leaving a 3 mm diameter opening. The body of the syringe (8 mm diameter) was cut so the total length was 10 mm. This well was mounted on a micromanipulator and lowered over the receptive field of each unit on the corium side (Figs. 1, 2B, C). A temperature probe was placed on the epidermal side in the receptive field. To apply cold stimulation, the SIF in the cylinder was gently pipetted out and a pellet of frozen SIF was placed very gently into the cylinder, avoiding any mechanical stimulation of the unit. These SIF pellets were made using a modified 1cc insulin syringe. The tip was cut off so that a 100 μl cylinder of frozen SIF could be pressed from the syringe and cut so that the shape and size was consistent from trial to trial. The syringes were stored in the freezer until needed. The frozen SIF pellets produced consistent cooling of the skin from 32 °C to 19 ± 1 °C in the first 3 s. By 6 s the temperature was within the noxious cold range at 16 °C; by 30 s it fell to about 9 °C. The temperature reached its nadir of about 7 °C by about 50 s, maintaining at 7 °C for another 30 s (measured on the epidermal side). A unit was considered cold-sensitive if the discharge rate evoked during cold stimulation was greater than the background mean frequency for that unit measured 30 s immediately preceding the cold stimulus [43]. To analyze temperature-dependent changes, we plotted the unit responses (in 3 s bins) of a subset of randomly selected units with at least a 1Hz response to cold stimulation.

2.7. Mechanical stimulation

A dual mode lever system (Aurora Scientific Inc., Ontario, Canada) was used to determine the mechanical threshold of each unit. The system had a motor-driven stylus (0.7 mm diameter) that delivered a force in the form of a continuous ascending ramp from 0 to 170 mN over 20 s. The stylus was placed on the corium side in the most sensitive region of the receptive field of the unit (Figs. 1, 2D). A unit was considered mechanically sensitive if the discharge rate evoked during stimulation was greater than the background mean frequency for that fiber during the 20 s immediately preceding the mechanical stimulus. The force eliciting the first spike upon activation of the ramp was considered threshold for that unit. A suprathreshold square wave pulse (180 mN, 10 s) was also applied. Firing rate during this stimulus was reported as the mechanical firing rate for that unit.

2.8. Cold tail-flick behavioral test

Changes in cold sensitivity were measured with the cold water tail-flick test. Mice were habituated for 4 days by placing them in cylindrical, plexiglass tubes with their tails exposed at the rear of the tube. On day 1 of habituation, mice were placed in the tubes for 25 min. On days 2–4, after 25 min in the tubes, the tails were immersed in room temperature water for 1 min to acclimate the tails to this sensation. On the following day, baseline tail flick latencies were determined. Mice were placed in the tubes for 15 min, then their tails were immersed for a maximum of 30 s in a mixture of equal parts water and ethanol cooled to −5 °C. The end point of the test occurred when the mice flicked their tails out of the water or reached the 30 s cut off. Each mouse was tested 3 times (5 min intervals), and the tail flick latencies were averaged to obtain a baseline. Animals were then injected with saline or morphine according to the protocol described above and retested ~12 h after the final morphine/saline injection. Average tail flick latencies were obtained using the same paradigm as on baseline days.

2.9. Statistical analyses

Data were expressed as means ± standard errors of means (SEM) and statistical analyses were performed using Prism software (GraphPad Software Inc., La Jolla, CA). In the electrophysiological studies, differences in discharge rates and thresholds were evaluated with either a Mann-Whitney, one-way ANOVA, or two-way repeated measures ANOVA. Differences in populations were evaluated with Fisher's exact test or z-test. For behavior studies, differences in populations were evaluated using the student's t-test. $P < 0.05$ was considered significant.

3. Results

3.1. Properties of fibers in the mouse skin-nerve preparation

The sciatic/tibial nerves (n = 6) from 3 naïve mice were used to measure conduction velocities from compound action potentials to further classify units as either C- or Aδ-fibers. Based on these measurements, the conduction velocity of C-fibers was estimated to be < 1.2 m/s and that of Aδ-fibers ≥ 1.2 m/s and < 10 m/s. This agrees with published literature using the mouse glabrous skin-nerve preparation [8].

Nociceptors were identified as high-threshold, slowly adapting mechanoreceptors with a conduction velocity (CV) between 0.2 and 10 m/s. Recordings were made from 126 nociceptors from 30 saline-treated (SAL) mice and 188 nociceptors from 26 morphine-treated (MOR) mice. Scattergrams were constructed for the nociceptor CV's from each population and there was no difference in the mean CV between the two populations (SAL fibers 2.7 ± 0.3 m/s, MOR fibers 2.9 ± 0.2 m/s; Mann-Whitney test; p = 0.26; Fig. 3A). Units were then parsed based on CV and for the SAL group 60 were classified as C-fibers (48%) and 66 as Aδ-fibers (52%). For the MOR group 72 were classified as C-fibers (38%) and 116 Aδ-fibers (61%). These numbers were not significantly different (Fisher's exact test; p = 0.10). The mean CV for C-fibers from MOR mice (0.7 ± 0.02 m/s) was not different from SAL mice (0.7 ± 0.03 m/s), nor was the distribution of the CVs different between the two groups (Fig. 3B). As seen in C-fibers, MOR treatment did not change the average CV of Aδ-fibers (4.0 ± 0.2 m/s MOR vs 3.6 ± 0.3 m/s SAL; p = 0.31), nor the distribution of CVs in SAL vs MOR (Fig. 3C).

One important change in MOR mice was the prevalence of nociceptors. The median number of nociceptive fibers in a MOR mouse, (7 per experiment) was significantly higher compared to that in a SAL mouse (4 per experiment, Mann-Whitney test; p < 0.05).

Specifically, the population of nociceptive Aδ-fibers was significantly larger (Mann-Whitney test; $p < 0.05$).

3.2. Morphine treatment increases background firing, afterdischarge and spontaneous activity (SA) in nociceptors

The mean background activity of all fibers during the first 2 min after a newly-teased filament was placed on the recording electrode was significantly higher in C-fibers from MOR compared to SAL mice (0.19 ± 0.04 vs. 0.04 ± 0.008 imp/s, respectively, Mann-Whitney test; $p < 0.005$, Fig. 4A). Aδ-fibers did not show this difference (0.02 ± 0.006 MOR vs. 0.01 ± 0.005 SAL, $p = 0.39$). In addition to the generally higher background firing of C-fibers, fibers from MOR mice showed episodes of aberrant activity throughout the recording sessions, which included afterdischarge and SA. Forty-one fibers (21.3%) from 18/26 MOR mice displayed such activity compared to only 3 fibers (2.3%) from 3/30 SAL mice (Fisher's exact test; $p < 0.0001$). The 41 MOR fibers included both C- (n=22/72; 30.6%) and Aδ-fibers (n=19/116; 16.4%), a proportion that was not significantly different (z-test; $p = 0.49$).

In MOR mice, 23 fibers (14 C- and 9 Aδ-fibers, Table 1) continued to respond after a stimulus was terminated or they displayed activity within 30 s after the termination of a stimulus. Either occurrence was judged to be induced by, or related to, the stimulus and categorized as afterdischarge. (This 30 s time frame was based on the histogram in Fig. 4B, which shows the propensity of aberrant events to begin within 30 s poststimulus, with an obvious break in activity between 30 and 60 s post-stimulus). These afterdischarge events were not triggered by a particular modality but could be observed after any stimulus (mechanical, heat, cold; Figs. 5A and B, 6A), could have a variable duration, with events lasting anywhere from 2 to 12 min (Figs. 5A and B, Table 1), have a mean frequency that was roughly one half of the rate evoked by the prior stimulus (Fig. 6B) and a peak firing rate that was no different from that evoked by the stimulus (Fig. 6C). Some MOR fibers had multiple afterdischarge events during a recording session (Fig. 5B). Afterdischarge was observed in only 2 C-fibers from SAL mice (Figs. 4B, 6A, Table 1).

Twenty six fibers (15 C and 11 Aδ) had aberrant SA that was unrelated to any stimulus (occurred at least 60 s after the end of a stimulus; Fig. 4B, Table 1). As with afterdischarge, some fibers had SA events multiple times during a recording session and the duration could be over 6 min (Table 1). There was no pattern to the generation of an SA event as one could occur at any time during the recording session: during the first interval prior to any stimulation (17 fibers) or in a timeframe ≥ 60 s following heat (13 fibers), cold (3 fibers) or mechanical (7 fibers) stimulation (Fig. 5C). Furthermore, the occurrence of SA was not related to fiber type (C- or Aδ-fiber; z-test; $p = 0.56$) or fiber responsiveness (heat, cold or mechanical). Only one C-fiber from SAL mice showed SA (Fig. 4B).

The firing pattern during an afterdischarge or SA event could be characterized as irregular, regular, or bursting based on the interspike interval [91]. A fiber could demonstrate one or more firing patterns at different points during the recording. Five fibers had periods of both irregular and regular firing, and one fiber had periods of irregular firing and bursting. Irregular firing patterns were the most common, characterized by slow, irregular activity with an average discharge rate of 0.9 ± 0.07 imp/s (Fig. 7A, Table 2). Fifteen C-fibers and 12 Aδ-fibers displayed this type of firing pattern. Aberrant activity occurring with a regular firing pattern (2.3 ± 0.3 imp/s; Fig. 7B, Table 2) was observed mainly during afterdischarge events in 10 fibers (5 C- and 5 Aδ-fibers) but only seen once during SA. An occasional burst could be seen interspersed with irregular and regular firing patterns. Six C-fibers and 3 Aδ-fibers showed aberrant activity containing more than 40% of the spikes in bursts (Fig. 7C). The overall firing rate for fibers during these events was 3.3 ± 0.9 imp/s and on average,

more than 70% of the spike activity occurred in bursts. The intraburst firing rate averaged 31.6 ± 8.2 imp/s (range 9.1 – 111.0 imp/s). There were no significant differences in the proportions of C- vs. Aδ-fibers in any of these categories (z-tests; $p > 0.05$). The 3 fibers from SAL mice showing SA all had an irregular firing pattern (0.7 ± 0.06 imp/s).

3.3. Morphine treatment increased the proportion of polymodal fibers concomitantly decreasing unimodal fibers

Typical responses of afferent fibers to stimuli are shown in Fig. 2. All fibers studied were mechano-sensitive since we used mechanical probing with a blunt glass rod to find units in the skin flap. Fibers that did not respond to either heating to 51°C or cooling to 7°C were classified as C- or Aδ-mechanical units (CM or AδM). Fibers that responded to heat stimuli were classified as C- or Aδ-mechano-heat units (CMH or AδMH) and those that responded to cold stimuli were classified as C- or Aδ-mechano-cold units (CMC or AδMC). Fibers that responded to both heat and cold were classified as C- or Aδ-mechano-heat-cold units (CMHC or AδMHC). A small population of fibers (n = 3 saline, 15 morphine) did not respond to cooling, but responded as the skin rewarmed (Fig. 2C). The warming response occurred in fibers that were (n = 5) and were not (n = 10) heat responsive. The population with this warming response was significantly larger in the MOR compared to SAL mice (Fisher's exact test; $p < 0.05$).

In SAL mice, 26.7% (16/60) of the C-fiber population was unimodal; i.e., they responded only to mechanical stimulation (Fig. 8A, Table 3). In MOR mice, this percentage was significantly decreased to 9.7% (7/72, Fisher's exact test; $p < 0.05$,), with corresponding increases in the percentages of polymodal CMH-, CMHC- and CMC-fibers; though individually, the increase in each category was not significant. Unimodal Aδ-fibers from SAL mice comprised 86.4% of the fiber population with the fibers responding to mechanical only. In MOR mice, this dropped to 60.3%, (Fisher's exact test; $p < 0.001$, Fig. 8A, Table 3), with a corresponding increase in polymodal fibers, rising from 13.6% to almost 40%. This change was due entirely to an increase in the population of AδMC's, which increased from 4.5% to 29.3% (Fisher's exact test; $p < 0.0001$, Table 3).

3.4. Morphine changed nociceptor responses to cold stimulation

Since only a few Aδ-fibers were responsive to cold in SAL mice, we combined C-and Aδ-fibers for analysis of cold responses. For nociceptors responsive to cold stimulation, there was no difference between the groups in firing rate (2.1 ± 0.2 imp/s MOR vs 2.7 ± 0.4 imp/s SAL; $p = 0.053$; Fig. 9B).

The threshold of activation to a cold stimulus was significantly lower (colder) in fibers from MOR mice (15.6 ± 0.8 °C) compared to SAL mice (21.2 ± 1.0 °C; $p < 0.001$; Fig. 9A). Since 2 populations of cold-receptive neurons have been identified in DRG culture experiments [5], we further subdivided the cold responsive fibers into those whose threshold fell into the range considered to be moderate cooling (17–26 °C) and noxious cold (<17 °C). These cool and cold sensations are thought to be mediated by TRPM8 and TRPA1, respectively [25]. There was no difference in the threshold of fibers activated by moderate cooling (22.3 ± 0.7 °C MOR vs. 21.5 ± 0.7 °C SAL; Fig. 9C) or in the firing rate of these fibers (3.5 ± 0.7 imp/s MOR vs. 3.3 ± 0.8 imp/s SAL; Fig. 9D). However, nociceptors activated in the noxious cold range from MOR mice had a significantly colder threshold (11.5 ± 0.4 °C) compared to fibers from SAL mice (13.6 ± 0.8 °C; $p < 0.05$; Fig. 9E). The firing rate was not different (1.5 ± 0.2 imp/s MOR vs 2.2 ± 0.5 imp/s SAL; $p = 0.20$; Fig. 9F).

For the cold sensitive C-fibers from SAL mice, there were 10 with thresholds in the moderate cooling range (17 – 26 °C), and 9 in the noxious cold range (< 17 °C). For MOR mice, there were 14 with thresholds in the moderate cooling range and 17 in the noxious cold range (Fig. 8B). Furthermore, the increase in the population of AδMC fibers was almost entirely in those fibers with thresholds in the noxious cold range. In the 4 cold-responsive Aδ-fibers from SAL mice where we obtained threshold data, 1 fiber was in the moderate cooling range and 3 in the noxious cold range. In MOR mice, there were 3 fibers with thresholds in the moderate cooling range and 27 in the noxious cold range (Fig. 8B).

In a subset of randomly selected units, cold responses were analyzed in more detail. At the onset of the cold stimulus, discharge rate rose sharply, remained elevated for 9 to 12 s and then began to adapt even as the temperature continued to fall (Fig. 10). For MOR mice, units with ongoing activity immediately preceding the cold stimulus had significantly higher temperature-dependent discharge rates compared to MOR units without ongoing activity (Figs. 10C, D). Furthermore, the responses were significantly heightened at 0 to 9 s and 12 to 15 s after initiation of the cold stimulus (Figs. 10C, D; two-way repeated measures ANOVA, df(1,19); $p < 0.05$). For SAL mice, there was also a significant temperature-dependent increase in discharge rate in response to cold stimulation and this type of response occurred in the presence or absence of ongoing activity (Figs. 10A, B).

3.5. Morphine did not change nociceptor responses to mechanical or heat stimulation

The threshold for C-fiber activation to mechanical stimulation in MOR mice (61.6 ± 4.5 mN) was not different from SAL mice (56.3 ± 5.1 mN; $p = 0.44$; Fig. 11A). Morphine treatment did not change the firing rate of C-fibers to suprathreshold mechanical stimulation (5.9 ± 0.8 imp/s MOR vs 6.1 ± 0.8 imp/s SAL; $p = 0.87$; Fig. 11B). The threshold for Aδ-fiber activation to a mechanical stimulus in MOR mice (70.3 ± 4.0 mN) was similar to that seen in SAL mice (65.7 ± 4.7 mN; $p = 0.47$; Fig. 11A). The firing rates to suprathreshold mechanical stimulation did not change in MOR mice (6.5 ± 0.5 m/s) vs. SAL mice (6.8 ± 0.7 m/s; $p = 0.76$; Fig. 11B). Only a few Aδ-fibers were responsive to heat. For that reason, we combined C- and Aδ-fibers for analysis of heat responses. There was no difference in heat threshold for nociceptors comparing MOR mice (40.1 ± 0.5 °C) to SAL mice (40.8 ± 0.7 °C; Fig. 11C) and the difference in firing rate between MOR (4.9 ± 0.6 imp/s) and SAL (3.7 ± 0.5 imp/s) was not significant ($p = 0.19$; Fig. 11D).

3.6. Morphine changed behavioral responses to cold stimulation

To determine if the robust increase in Aδ-fibers sensitive to cold was functionally relevant, the cold water (−5 °C) tail flick latency test was performed on a separate group of MOR and SAL mice (n = 20; 10/group). Pre-drug tail flick latencies (21.3 ± 2.2 s) were obtained and the animals retested ~12 h after the final morphine injection. The MOR mice displayed a marked cold sensitivity with the tail flick latencies shortened to 17.6 ± 2.8 s compared to 24.1 ± 2.3 s in SAL mice. When expressed as percentage of baseline, MOR mice showed a 34.4 ± 15.6% decrease in tail flick latency compared to a 8.1% increase in the SAL mice (student's t-test; $p < 0.05$, Fig. 12).

4. Discussion

This study demonstrates for the first time, changes in nociceptor activity and sensitivity resulting from repeated systemic MOR treatment. The aberrant activity observed in cutaneous nociceptors in MOR but not SAL mice includes elevated background firing activity in C-fibers at "rest", afterdischarge and SA in both C- and Aδ-fibers. MOR treatment increases the proportion of fibers displaying polymodal responses compared to that with mechanical-only responses. This change in proportion is related to a significant

increase in the percentage of cold sensitive Aδ-fibers, which results in functional consequences since behavioral testing demonstrates that MOR mice develop cold sensitivity.

4.1. Morphine produces aberrant activity in nociceptors

MOR treatment is associated with aberrant activity in C and Aδ nociceptors, consisting of afterdischarge and SA. Both types of aberrant activity include irregular, regular, or bursting patterns. Irregular is most commonly seen by us and reported by others in sensory neurons [3,84,91]. There are many reports of SA in primary afferents in various animal pain models including peripheral neuropathy [2,30,41,46,77,79,93], inflammation [30,35,36,49,53,90], skin incision [8,92], and spinal cord injury [9,15]. However, reports of afterdischarge in primary afferents are rare and have been related to mechanical stimulation [50,85] or step depolarization [67]. Nociceptors in MOR mice show afterdischarge in response to all modalities tested (mechanical, heat and cold). As shown in animal studies, increased firing frequency is related to increased release of amino acids, neuropeptides and/or neurotrophins, agents that can produce/amplify pain signals. For example, peripheral glutamate increases following nerve activity [28,48] and activates nociceptors [16,35,36]. C-fiber activity can increase substance P (SP) release in the periphery [1], and this elevation produces nociceptive behaviors [17] and sensitization of afferents [39]. Importantly, knock out of the preprotachykinin A gene encoding for SP reduces mechanical allodynia that develops in MOR mice [71]. Brainderived neurotrophic factor (BDNF) is released during bursting activity [56], and can induce cold allodynia [24] and contribute to mechanical allodynia [64,94], two sensory abnormalities demonstrated in the MOR mice [12].

We hypothesize that this aberrant afferent activity is one mechanism underlying pain behaviors in MOR mice and OIH in patients. Human microneurography studies show that nociceptor discharge rates ≥ 0.4 ± 1.0 imp/s can be perceived as painful [73,83]. The average discharge rate we observe in irregular firing in MOR mice is 0.9 ± 0.07 imp/s, and for regular and bursting patterns, rates are far higher (≥ 2.3 imp/s). Microneurography in neuropathic pain patients reveals afterdischarge and spontaneous ectopic discharges [13], firing patterns we observe in nociceptors in MOR mice. During spontaneous discharge of C-fibers, patients experience spontaneous pain. A reduction in C-mechanoreceptor thresholds and repetitive discharge in humans is associated with experiences of hyperalgesia/allodynia [65]. Hence, it is highly likely that the aberrant activity we observe in C and Aδ nociceptors contributes to the pain state in MOR mice.

Chronic opioid administration causes hyperexitability at the level of the DRG. *In vitro* cultures of hybrid neuroblastoma - DRG cells and explant DRG cultures show that chronic opioid exposure results in supersensitivity manifest as a prolongation of the action potential duration [26,89]. In DRGs from mice chronically implanted with morphine pellets, enhanced neuronal excitability is demonstrated by an increase in the number of action potentials at 2X the rheobase current [69]. Regardless of these MOR-induced changes, DRG cells bodies are clearly not the source of activity we observe since afferents are disconnected from the DRG cell bodies in our *in vitro* skin-nerve preparation, Thus, an opioid-induced neuroplasticity has occurred in the sensory neurons that is readily detected in the peripheral fibers and maintained *in vitro*.

Aberrant activity is also found in the spinal cord after chronic morphine. Compared to saline controls, dorsal horn neurons show dose-dependent increases in responses to Aδ- and C-fiber input driven either electrically or by natural mechanical stimulation in the periphery [80]. Wind-up, an intrinsic spinal event mediated via postsynaptic mechanisms, is not seen. The lack of wind-up supports the idea that alterations in nociceptive fibers can be a driving force for opioid-induced sensory abnormalities. One caveat is that peripheral nociceptors do not show any change in mechanical threshold or in discharge rate to a suprathreshold

mechanical stimulus, but mechanical allodynia is reported in mice using this same morphine treatment paradigm [6,12]. This suggests that changes in mechanical sensitivity are related either to input from non-nociceptors (were not recorded from) or to central changes as described above (i.e. central sensitization) [55,58,87,88].

4.2. Silent nociceptors may contribute to OIH

Another intriguing finding in this study is that nociceptors are more prevalent in MOR compared to SAL mice. We propose that this increase in fibers in MOR mice is due to activation of previously silent nociceptors. Silent nociceptors or mechanically insensitive afferents (MIAs) have been directly observed in a feline arthritis model where units that were previously silent began to show activity in response to mechanical stimulation after inflammation [75]. It has been reported that MIAs constitute a special class of fibers that require tissue damage/inflammation for excitement [18,75]. The fact that nociceptive fibers are significantly easier to find with a mechanical search stimulus in MOR mice suggests that MIAs are no longer insensitive following chronic MOR treatment. This is reflected in the change in the number of fibers that become mech-only sensitive and mech-cold sensitive in MOR vs SAL mice (Table 3). Since MIA's are a large percentage of the population of cutaneous nociceptors (20 – 50% [60]), their activation would greatly amplify the total nociceptive input transmitted to the CNS. The apparent activation of silent nociceptors by morphine in the absence of injury or inflammation could send a false injury signal to the CNS and thus contribute to the generation of OIH.

4.3. Morphine treatment induces hypersensitivity to cold

Increased cold sensitivity is reported in other rodent models including inflammation and neuropathic pain [10,19,33,43,44]; however, this is the first report in morphine-treated rodents. The increased proportion of cold sensitive Aδ-fibers correlates well with the increased cold sensitivity observed in the MOR mice. In contrast, the same morphine paradigm does not produce increased sensitivity in a variety of heat tests [6,12].

In studies spanning 5 decades, cold hypersensitivity is consistently the most robust sensory abnormality related to OIH in addicts and volunteers taking opioids [22,23,31,32,38,40,59,66,76]. Reports of hypersensitivity to heat, mechanical or electrical stimulation is equivocal or absent. It is suggested that the specific sensitivity to cold pain in addicts is not a physiological symptom but a psychological one [20,68]. Our data suggests a physiological basis due to robust temperature-dependent differences in nociceptor sensitivity to cold, increases in the population of cold-sensitive Aδ-fibers (AδMC), and behavioral evidence that MOR mice are more sensitive to cold. Additionally, the increase in AδMC responsive fibers is primarily in the population responsive to noxious cold (< 17 °C). This would presumably decrease the ability to tolerate colder temperatures. Paradoxically, we find that AδMC nociceptors begin to fire at colder temperatures (higher threshold) in MOR compared to SAL mice. In some human studies, addicts do not report cold pain until lower temperatures are reached [57,66]. These results correlate more closely with our results showing a colder threshold in nociceptors. Studies universally show that pain tolerance is reduced in opioid-using groups. Lowered tolerance could occur because once the temperature is low enough to activate the AδMCs, more are available to be recruited in MOR mice, possibly decreasing tolerance to cold. Noxious cold sensation (< 17 °C) is thought to be mediated at least partially by TRPA1 [25]. Upregulation of TRPA1 parallels the development of cold allodynia in nerve injured rats and is alleviated by TRPA1 anti-sense RNA [47,63]. Thus, it is possible MOR treatment up-regulates TRPA1 mRNA.

Reports suggest that TREK-1 and TRAAK K+ channels work in tandem with excitatory thermo-TRP channels, setting temperature threshold, range and intensity of nociceptor

excitation [29,62]. On the other hand, cold temperatures (<15 °C) inhibit A-type K+ currents. These currents function as 'brakes' to counteract membrane depolarization [74], reducing nociceptor hyperexcitability. Thus, if noxious cold inhibits these currents, this could facilitate action potential firing with little or no involvement of TRPA1 activity. Therefore, contributions of K+ channels cannot be ruled out in the interpretation of our results.

4.4 Conclusion

This MOR paradigm results in significant changes in nociceptor function including: 1) increased background activity in C-fibers, 2) afterdischarge following mechanical, heat or cold stimulation, 3) SA in C- and Aδ-fibers; 4) an increased prevalence of AδMC's suggesting either a change in phenotype in the Aδ population (AδM becoming AδMC) or recruitment of MIAs that have cold thresholds in the noxious range (<17 °C), thus recruitment of mechanically- and cold-insensitive afferents (MCIAs). The latter has functional consequences, producing an increased sensitivity to cold in a behavioral assay. It is possible that morphine treatment leads to subthreshold membrane potential oscillations in nociceptors [3,67] that can give rise to all/any of the aberrant activity we describe. Similar changes in nociceptor activity and nociceptor phenotype in patients on long term or high dose opioids could be interpreted as painful and are likely to be mechanisms underlying OIH.

Acknowledgments

These studies were supported by NIH DA027460 and NS 027910 to SMC, DA032298 to ALB, and DA027460 and DA025036 to JAM.

References

1. Adelson D, Lao L, Zhang G, Kim W, Marvizón JCG. Substance P release and neurokinin 1 receptor activation in the rat spinal cord increase with the firing frequency of C-fibers. Neurosci. 2009; 161:538–553.
2. Amir R, Devor M. Ongoing activity in neuroma afferents bearing retrograde sprouts. Brain Res. 1993; 630:283–288. [PubMed: 8118694]
3. Amir R, Michaelis M, Devor M. Burst discharge in primary sensory neurons: triggered by subthreshold oscillations, maintained by depolarizing afterpotentials. J Neurosci. 2002; 22:1187–1198. [PubMed: 11826148]
4. Angst MS, Clark JD. Opioid-induced hyperalgesia: a qualitative systematic review. Anesthesiol. 2006; 104:570–587.
5. Babes A, Zorzon D, Reid G. Two populations of cold-sensitive neurons in rat dorsal root ganglia and their modulation by nerve growth factor. Eur J Neurosci. 2004; 20:2276–2282. [PubMed: 15525269]
6. Baker A, Zhou S, Hargett G, Moron Concepcion J, Carlton S. Morphine induces pain behavior and iGluR4 upregulation in murine spinal cord. J Pain. 2011; 12:39.
7. Ballantyne JC, Mao J. Opioid therapy for chronic pain. New Eng J Med. 2003; 349:1943–1953. [PubMed: 14614170]
8. Banik RK, Brennan TJ. Sensitization of primary afferents to mechanical and heat stimuli after incision in a novel in vitro mouse glabrous skin-nerve preparation. Pain. 2008; 138:380–391. [PubMed: 18316159]
9. Bedi SS, Yang Q, Crook RJ, Du J, Wu Z, Fishman HM, Grill RJ, Carlton SM, Walters ET. Chronic spontaneous activity generated in the somata of primary nociceptors is associated with pain-related behavior after spinal cord injury. J Neurosci. 2010; 30:14870–14882. [PubMed: 21048146]
10. Brenner DS, Golden JP, Gereau RWIV. A Novel Behavioral Assay for Measuring Cold Sensation in Mice. PLoS One. 2012; 7:e39765. [PubMed: 22745825]

11. Bull P, Russell J, Scott V, Brown C. Apamin increases post-spike excitability of supraoptic nucleus neurons in anaesthetized morphine-naïve rats and morphine-dependent rats: consequences for morphine withdrawal excitation. Exp Brain Res. 2011; 212:517–528. [PubMed: 21671103]
12. Cabanero D, Baker A, Zhou S, Hargett GL, Irie T, Xia Y, Beaudry H, Gendron L, Melyan Z, Carlton SM, Moron JA. Pain after discontinuation of morphine treatment Is associated with synaptic increase of GluA4-containing AMPAR in the dorsal horn of the spinal cord. Neuropsychopharmacol. 2013 [Epub ahead of print].
13. Campero M, Serra J, Marchettini P, Ochoa JL. Ectopic impulse generation and autoexcitation in single myelinated afferent fibers in patients with peripheral neuropathy and positive sensory symptoms. Muscle Nerve. 1998; 21:1661–1667. [PubMed: 9843066]
14. Carlton SM, Coggeshall RE. Immunohistochemical localization of enkephalin in peripheral sensory axons in the rat. Neurosci Lett. 1997; 221:121–124. [PubMed: 9121679]
15. Carlton SM, Du J, Tan HY, Nesic O, Hargett GL, Bopp AC, Yamani A, Lin Q, Willis WD, Hulsebosch CE. Peripheral and central sensitization in remote spinal cord regions contribute to central neuropathic pain after spinal cord injury. Pain. 2009; 147:265–276. [PubMed: 19853381]
16. Carlton SM, Hargett GL, Coggeshall RE. Localization and activation of glutamate receptors in unmyelinated axons of rat glabrous skin. Neurosci Lett. 1995; 197:25–28. [PubMed: 8545047]
17. Carlton SM, Zhou S, Coggeshall RE. Evidence for the interaction of glutamate and NK1 receptors in the periphery. Brain Res. 1998; 790:160–169. [PubMed: 9593874]
18. Cervero F, Jänig W. Visceral nociceptors: a new world order? Trends Neurosci. 1992; 15:374–378. [PubMed: 1279857]
19. Choi Y, Yoon YW, Na HS, Kim SH, Chung JM. Behavioral signs of ongoing pain and cold allodynia in a rat model of neuropathic pain. Pain. 1994; 59:369–376. [PubMed: 7708411]
20. Chu LF, Angst MS, Clark D. Opioid-induced hyperalgesia in humans: molecular mechanisms and clinical considerations. Clin J Pain. 2008; 24:479–496. [PubMed: 18574358]
21. Coggeshall RE, Zhou S, Carlton SM. Opioid receptors on peripheral sensory axons. Brain Res. 1997; 764:126–132. [PubMed: 9295201]
22. Compton MA. Cold-pressor pain tolerance in opiate and cocaine abusers: correlates of drug type and use status. J Pain Symptom Manag. 1994; 9:462–473.
23. Compton P, Charuvastra VC, Ling W. Pain intolerance in opioid-maintained former opiate addicts: effect of long-acting maintenance agent. Drug Alcohol Depen. 2001; 63:139–146.
24. Constandil L, Goich M, Hernandez A, Bourgeais L, Cazorla M, Hamon M, Villanueva L, Pelissier T. Cyclotraxin-B, a new TrkB antagonist, and glial blockade by propentofylline, equally prevent and reverse cold allodynia induced by BDNF or partial infraorbital nerve constriction in mice. J Pain. 2012; 13:579–589. [PubMed: 22560237]
25. Cortright DN, Krause JE, Broom DC. TRP channels and pain. BBA-Mol Basis Dis. 2007; 1772:978–988.
26. Crain SM, Shen KF. After chronic opioid exposure sensory neurons become supersensitive to the excitatory effects of opioid agonists and antagonists as occurs after acute elevation of GM1 ganglioside. Brain Res. 1992; 575:13–24. [PubMed: 1324084]
27. Crofford LJ. Adverse effects of chronic opioid therapy for chronic musculoskeletal pain. Nat Rev Rheumatol. 2010; 6:191–197. [PubMed: 20357788]
28. deGroot J, Zhou S, Carlton SM. Peripheral glutamate release in the hindpaw following low and high intensity sciatic stimulation. Neuroreport. 2000; 11:497–502. [PubMed: 10718302]
29. Descoeur J, Pereira V, Pizzoccaro A, Francois A, Ling B, Maffre V, Couette B, Busserolles J, Courteix C, Noel J, Lazdunski M, Eschalier A, Authier N, Bourinet E. Oxaliplatininduced cold hypersensitivity is due to remodelling of ion channel expression in nociceptors. EMBO Mol Med. 2011; 3:266–278. [PubMed: 21438154]
30. Djouhri L, Koutsikou S, Fang X, McMullan S, Lawson SN. Spontaneous pain, both neuropathic and inflammatory, is related to frequency of spontaneous firing in intact C-fiber nociceptors. J Neurosci. 2006; 26:1281–1292. [PubMed: 16436616]
31. Doverty M, Somogyi AA, White JM, Bochner F, Beare CH, Menelaou A, Ling W. Methadone maintenance patients are cross-tolerant to the antinociceptive effects of morphine. Pain. 2001; 93:155–163. [PubMed: 11427327]

32. Doverty M, White JM, Somogyi AA, Bochner F, Ali R, Ling W. Hyperalgesic responses in methadone maintenance patients. Pain. 2001; 90:91–96. [PubMed: 11166974]
33. Dowdall T, Robinson I, Meert TF. Comparison of five different rat models of peripheral nerve injury. Pharmacol Biochem Behav. 2005; 80:93–108. [PubMed: 15652385]
34. Du J, Koltzenburg M, Carlton SM. Glutamate-induced excitation and sensitization of nociceptors in rat glabrous skin. Pain. 2001; 89:187–198. [PubMed: 11166475]
35. Du J, Zhou S, Carlton SM. Kainate-induced excitation and sensitization of nociceptors in normal and inflamed rat glabrous skin. Neurosci. 2006; 137:999–1013.
36. Du J, Zhou S, Coggeshall RE, Carlton SM. N-methyl-D-aspartate-induced excitation and sensitization of normal and inflamed nociceptors. Neurosci. 2003; 118:547–562.
37. Georges F, Aston-Jones G. Prolonged activation of mesolimbic dopaminergic neurons by morphine withdrawal following clonidine: participation of imidazoline and norepinephrine receptors. Neuropsychopharmacol. 2003; 28:1140–1149.
38. Hay JL, White JM, Bochner F, Somogyi AA, Semple TJ, Rounsefell B. Hyperalgesia in opioid-managed chronic pain and opioid-dependent patients. J Pain. 2009; 10:316–322. [PubMed: 19101210]
39. Heppelmann B, Pawlak M. Sensitisation of articular afferents in normal and inflamed knee joints by substance P in the rat. Neurosci Lett. 1997; 223:97–100. [PubMed: 9089682]
40. Ho A, Dole VP. Pain perception in drug-free and in methadone-maintained human exaddicts. P Soc Exp Biol Med. 1979; 162:392–395.
41. Hu S-J, Xing J-L. An experimental model for chronic compression of dorsal root ganglion produced by intervertebral foramen stenosis in the rat. Pain. 1998; 77:15–23. [PubMed: 9755014]
42. Jalabert M, Bourdy R, Courtin J, Veinante P, Manzoni OJ, Barrot M, Georges Fo. Neuronal circuits underlying acute morphine action on dopamine neurons. PNAS. 2011; 108:16446–16450. [PubMed: 21930931]
43. Ji G, Zhou S, Kochukov MY, Westlund KN, Carlton SM. Plasticity in intact A delta- and C-fibers contributes to cold hypersensitivity in neuropathic rats. Neurosci. 2007; 150:182–193.
44. Jørum E, Warncke T, Stubhaug A. Cold allodynia and hyperalgesia in neuropathic pain: the effect of N-methyl-d-aspartate (NMDA) receptor antagonist ketamine, a double-blind, cross-over comparison with alfentanil and placebo. Pain. 2003; 101:229–235. [PubMed: 12583865]
45. Joseph EK, Levine JD. Mu and delta opioid receptors on nociceptors attenuate mechanical hyperalgesia in rat. Neuroscience. 2010; 171:344–350. [PubMed: 20736053]
46. Kajander KC, Bennett GJ. Onset of a painful peripheral neuropathy in rat: a partial and differential deafferentation and spontaneous discharge in A beta and A delta primary afferent neurons. J Neurophysiol. 1992; 68:734–744. [PubMed: 1331353]
47. Katsura H, Obata K, Mizushima T, Yamanaka H, Kobayashi K, Dai Y, Fukuoka T, Tokunaga A, Sakagami M, Noguchi K. Antisense knock down of TRPA1, but not TRPM8, alleviates cold hyperalgesia after spinal nerve ligation in rats. Exp Neurol. 2006; 200:112–123. [PubMed: 16546170]
48. Kawamata T, Omote K. Activation of spinal N-methyl-D-aspartate receptors stimulates a nitric oxide/cyclic guanosine 3,5-monophosphate/glutamate release cascade in nociceptive signaling. Anesthesiol. 1999; 91:1415–1424.
49. Kelly S, Dunham JP, Murray F, Read S, Donaldson LF, Lawson SN. Spontaneous firing in C-fibers and increased mechanical sensitivity in A-fibers of knee joint-associated mechanoreceptive primary afferent neurones during MIA-induced osteoarthritis in the rat. Osteoarthr Cartilage. 2012; 20:305–313.
50. Kitagawa J, Takeda M, Suzuki I, Kadoi J, Tsuboi Y, Honda K, Matsumoto S, Nakagawa H, Tanabe A, Iwata K. Mechanisms involved in modulation of trigeminal primary afferent activity in rats with peripheral mononeuropathy. Eur J Neurosci. 2006; 24:1976–1986. [PubMed: 17040479]
51. Kolesnikov Y, Pasternak GW. Topical opioids in mice: analgesia and reversal of tolerance by a topical N-methyl-D-aspartate antagonist. J Pharmacol Exp Ther. 1999; 290:247–252. [PubMed: 10381783]

52. Kolesnikov YA, Jain S, Wilson R, Pasternak GW. Peripheral morphine analgesia: synergy with central sites and a target of morphine tolerance. J Pharmacol Exp Ther. 1996; 279:502–506. [PubMed: 8930151]
53. Koltzenburg M, Bennett DLH, Shelton DL, McMahon SB. Neutralization of endogenous NGF prevents the sensitization of nociceptors supplying inflamed skin. Eur J Neurosci. 1999; 11:1698–1704. [PubMed: 10215923]
54. Kumazawa T, Mizumura K, Sato J, Minagawa M. Facilitatory effects of opioids on the discharges of visceral nociceptors. Brain Research. 1989; 497:231–238. [PubMed: 2573404]
55. LaMotte RH, Shain CN, Simone DA, Tsai EF. Neurogenic hyperalgesia: psychophysical studies of underlying mechanisms. J Neurophysiol. 1991; 66:190–211. [PubMed: 1919666]
56. Lever IJ, Bradbury EJ, Cunningham JR, Adelson DW, Jones MG, McMahon SB, Marvizon JC, Malcangio M. Brain-derived neurotrophic factor is released in the dorsal horn by distinctive patterns of afferent fiber stimulation. J Neurosci. 2001; 21:4469–4477. [PubMed: 11404434]
57. Liebmann PM, Lehofer M, Moser M, Hoehn-Saric R, Legl T, Pernhaupt G, Schauenstein K. Persistent analgesia in former opiate addicts is resistant to blockade of endogenous opioids. Biol Psych. 1997; 42:962–964.
58. Mantyh PW, Rogers SD, Honore P, Allen BJ, Ghilardi JR, Li J, Daughters RS, Lappi DA, Wiley RG, Simone DA. Inhibition of hyperalgesia by ablation of lamina I spinal neurons expressing the substance P receptor. Science. 1997; 278:275–279. [PubMed: 9323204]
59. Martin JE, Inglis J. Pain tolerance and narcotic addiction. Brit J Social Clin Psychol. 1965; 4:224–229.
60. Michaelis M, Habler HJ, Janig W. Silent afferents: a separate class of primary afferents? Clin Exp Pharmacol Physiol. 1996; 23:99–105. [PubMed: 8819636]
61. Moron JA, Abul-Husn NS, Rozenfeld R, Dolios G, Wang R, Devi LA. Morphine administration alters the profile of hippocampal postsynaptic density-associated proteins: a proteomics study focusing on endocytic proteins. Mol Cell Prot. 2007; 6:29–42.
62. Noel J, Zimmermann K, Busserolles J, Deval E, Alloui A, Diochot S, Guy N, Borsotto M, Reeh P, Eschalier A, Lazdunski M. The mechano-activated K+ channels TRAAK and TREK-1 control both warm and cold perception. EMBO J. 2009; 28:1308–1318. [PubMed: 19279663]
63. Obata K, Katsura H, Mizushima T, Yamanaka H, Kobayashi K, Dai Y, Fukuoka T, Tokunaga A, Tominaga M, Noguchi K. TRPA1 induced in sensory neurons contributes to cold hyperalgesia after inflammation and nerve injury. J Clin Invest. 2005; 115:2393–2401. [PubMed: 16110328]
64. Obata N, Mizobuchi S, Itano Y, Matsuoka Y, Kaku R, Tomotsuka N, Morita K, Kanzaki H, Ouchida M, Yokoyama M. Decoy strategy targeting the brain-derived neurotrophic factor exon I to attenuate tactile allodynia in the neuropathic pain model of rats. Biochem Biophys Res Commun. 2011; 408:139–144. [PubMed: 21466785]
65. Ochoa JL, Campero M, Serra J, Bostock H. Hyperexcitable polymodal and insensitive nociceptors in painful human neuropathy. Muscle Nerve. 2005; 32:459–472. [PubMed: 15973653]
66. Pud D, Cohen D, Lawental E, Eisenberg E. Opioids and abnormal pain perception: New evidence from a study of chronic opioid addicts and healthy subjects. Drug Alcohol Depen. 2006; 82:218–223.
67. Radtke C, Vogt PM, Devor M, Kocsis JD. Keratinocytes acting on injured afferents induce extreme neuronal hyperexcitability and chronic pain. Pain. 2010; 148:94–102. [PubMed: 19932564]
68. Rainville P, Feine JS, Bushnell MC, Duncan GH. A psychophysical comparison of sensory and affective responses to four modalities of experimental pain. Somatosens Motor Res. 1992; 9:265–277.
69. Ross GR, Gade AR, Dewey WL, Akbarali HI. Opioid-induced hypernociception is associated with hyperexcitability and altered tetrodotoxin-resistant Na+ channel function of dorsal root ganglia. Amer J Physiol - Cell Physiol. 2012; 302:C1152–C1161. [PubMed: 22189556]
70. Russell NJ, Schaible HG, Schmidt RF. Opiates inhibit the discharges of fine afferent units from inflamed knee joint of the cat. Neurosci Lett. 1987; 76:107–112. [PubMed: 2884605]
71. Sahbaie P, Shi X, Li X, Liang D, Guo TZ, Qiao Y, Yeomans DC, Kingery WS, David Clark J. Preprotachykinin-a gene disruption attenuates nociceptive sensitivity after opioid administration

and incision by peripheral and spinal mechanisms in mice. J Pain. 2012; 13:997–1007. [PubMed: 23031399]

72. Sandkühler J. Models and mechanisms of hyperalgesia and allodynia. Physiol Rev. 2009; 89:707–758. [PubMed: 19342617]
73. Sang CN, Max MB, Gracely RH. Stability and reliability of detection thresholds for human A-Beta and A-delta sensory afferents determined by cutaneous electrical stimulation. J Pain Symptom Manag. 2003; 25:64–73.
74. Sarria I, Ling J, Gu JG. Thermal sensitivity of voltage-gated Na+ channels and A-type K+ channels contributes to somatosensory neuron excitability at cooling temperatures. J Neurochem. 2012; 122:1145–1154. [PubMed: 22712529]
75. Schaible HG, Schmidt RF. Time course of mechanosensitivity changes in articular afferents during a developing experimental arthritis. J Neurophysiol. 1988; 60:2180–2195. [PubMed: 3236065]
76. Schall U, Katta T, Pries E, Kloppel A, Gastpar M. Pain perception of intravenous heroin users on maintenance therapy with levomethadone. Pharmacopsych. 1996; 29:176–179.
77. Serra J, Bostock H, Solà R, Aleu J, García E, Cokic B, Navarro X, Quiles C. Microneurographic identification of spontaneous activity in C-nociceptors in neuropathic pain states in humans and rats. Pain. 2012; 153:42–55. [PubMed: 21993185]
78. Stein C, Hassan AH, Przewlocki R, Gramsch C, Peter K, Herz A. Opioids from immunocytes interact with receptors on sensory nerves to inhibit nociception in inflammation. PNAS. 1990; 87:5935–5939. [PubMed: 1974052]
79. Study RE, Kral MG. Spontaneous action potential activity in isolated dorsal root ganglion neurons from rats with a painful neuropathy. Pain. 1996; 65:235–242. [PubMed: 8826512]
80. Suzuki R, Porreca F, Dickenson AH. Evidence for spinal dorsal horn hyperexcitability in rats following sustained morphine exposure. Neurosci Lett. 2006; 407:156–161. [PubMed: 16959420]
81. Taylor BK, Peterson MA, Roderick RE, Tate J, Green PG, Levine JO, Basbaum AI. Opioid inhibition of formalin-induced changes in plasma extravasation and local blood flow in rats. Pain. 2000; 84:263–270. [PubMed: 10666531]
82. Tompkins DA, Campbell CM. Opioid-induced hyperalgesia: clinically relevant or extraneous research phenomenon? Curr Pain Headache Rep. 2011; 15:129–136. [PubMed: 21225380]
83. Van Hees J, Gybels J. C nociceptor activity in human nerve during painful and non painful skin stimulation. J Neurol Neurosurg Psych. 1981; 44:600–607.
84. Wall PD, Devor M. Sensory afferent impulses originate from dorsal root ganglia as well as from the periphery in normal and nerve injured rats. Pain. 1983; 17:321–339. [PubMed: 6664680]
85. Weng X, Smith T, Sathish J, Djouhri L. Chronic inflammatory pain is associated with increased excitability and hyperpolarization-activated current (Ih) in C- but not Adelta-nociceptors. Pain. 2012; 153:900–914. [PubMed: 22377439]
86. Wenk HN, Brederson JD, Honda CN. Morphine directly inhibits nociceptors in inflamed skin. J Neurophysiol. 2006; 95:2083–2097. [PubMed: 16339007]
87. Woolf CJ. Evidence for a central component of post-injury pain hypersensitivity. Nature. 1983; 306:686–688. [PubMed: 6656869]
88. Woolf CJ. Central sensitization: implications for the diagnosis and treatment of pain. Pain. 2011; 152:S2–S15. [PubMed: 20961685]
89. Wu G, Fan SF, Lu ZH, Ledeen RW, Crain SM. Chronic opioid treatment of neuroblastoma X dorsal root ganglion neuron hybrid F11 cells results in elevated GM1 ganglioside and cyclic adenosine monophosphate levels and onset of naloxoneevoked decreases in membrane K+ currents. J Neurosci Res. 1995; 42:493–503. [PubMed: 8568936]
90. Xiao W-H, Bennett GJ. Persistent low-frequency spontaneous discharge in A-fiber and C-fiber primary afferent neurons during an “inflammatory pain condition. Anesthesiol. 2007; 107:813–821.
91. Xie W, Strong JA, Kim D, Shahrestani S, Zhang JM. Bursting activity in myelinated sensory neurons plays a key role in pain behavior induced by localized inflammation of the rat sensory ganglion. Neurosci. 2012; 206:212–223.
92. Xu J, Brennan TJ. Comparison of skin incision vs. skin plus deep tissue incision on ongoing pain and spontaneous activity in dorsal horn neurons. Pain. 2009; 144:329–339. [PubMed: 19527922]

93. Zhang J-M, Song X-J, LaMotte RH. Enhanced excitability of sensory neurons in rats with cutaneous hyperalgesia produced by chronic compression of the dorsal root ganglion. J Neurophysiol. 1999; 82:3359–3366. [PubMed: 10601467]

94. Zhang X, Xu Y, Wang J, Zhou Q, Pu S, Jiang W, Du D. The effect of intrathecal administration of glial activation inhibitors on dorsal horn BDNF overexpression and hind paw mechanical allodynia in spinal nerve ligated rats. J Neural Trans. 2012; 119:329–336.

95. Zimmermann M. Ethical guidelines for investigations of experimental pain in conscious animals. Pain. 1983; 16:109–110. [PubMed: 6877845]

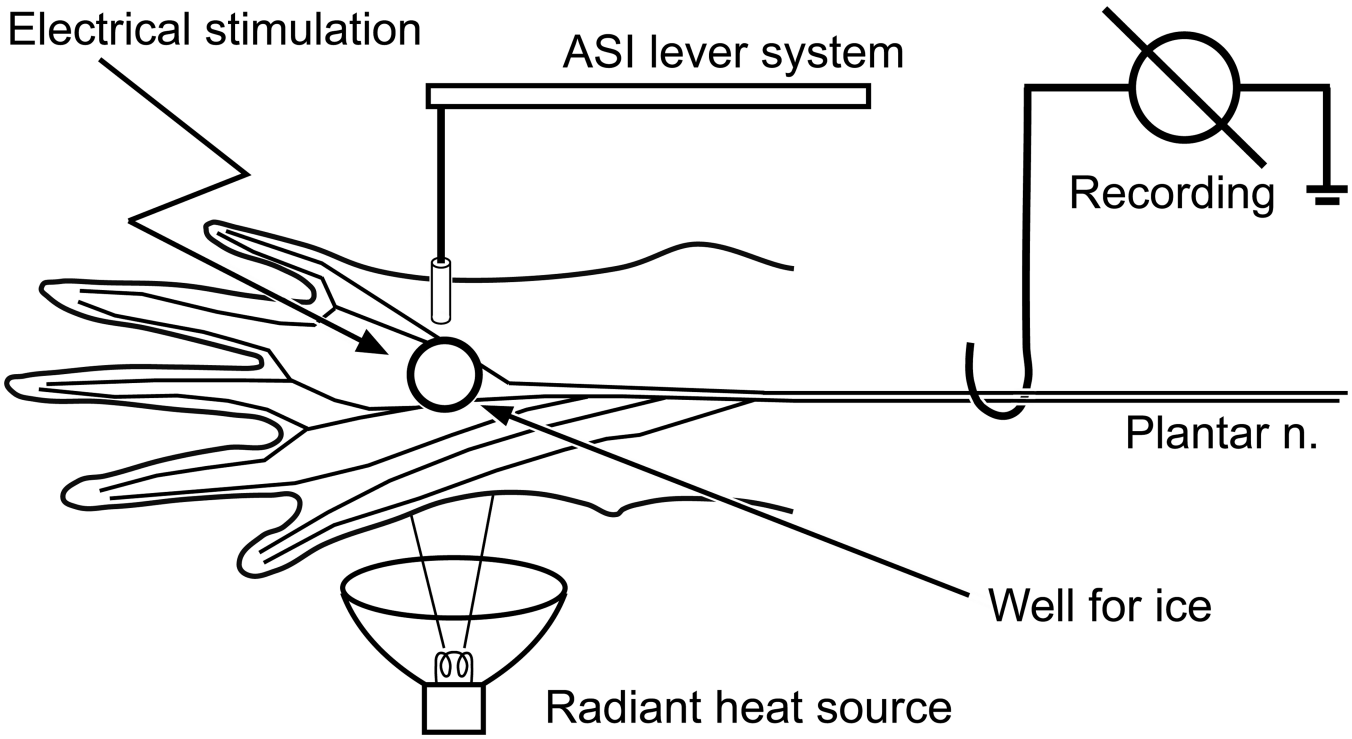

Figure 1.
Schematic drawing of the mouse skin-nerve preparation. Heat (radiant), cold (ice), and mechanical (lever system) stimulation is applied sequentially to the skin with 5 min rest periods in between each stimulus. At the end of the recording period, electrical stimulation of the receptive field is used to obtain a latency to calculate conduction velocity.

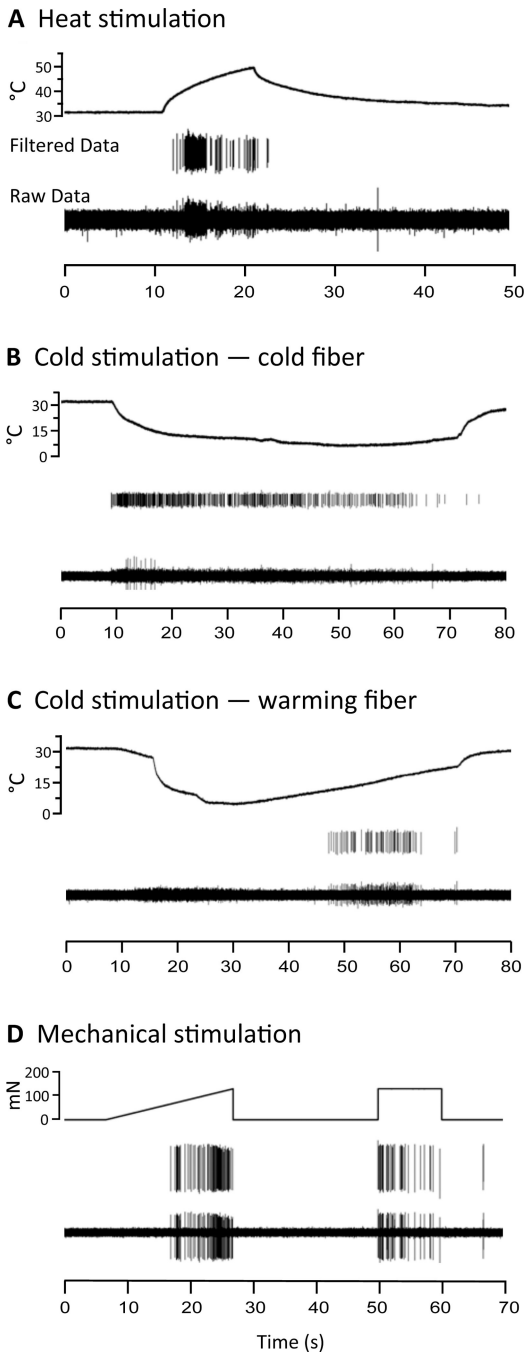

Figure 2.

Examples of standard stimuli and unit responses. For all panels, upper trace shows stimulation parameters, middle trace shows data filtered for the unit of interest using Spike2's template matching for spike sorting, and bottom trace shows raw data for that unit. A) Heat: A radiant heat source delivers a 10 s heat stimulus, which starts at 32 °C and increases to 51 °C. B) Cold: Starting from 32 °C, a uniform ice pellet (cylinder-shaped) cools the skin to 7 °C. C) Warming: The stimulus is the same as in C, but the unit does not start firing until the skin begins to warm up from the minimum 7 °C temperature. D) Mechanical: A computer driven ramp stimulus determines mechanical threshold, ascending

from 0 to 170 mN over 20 s. A square wave stimulus measures activity to a suprathreshold stimulus of 180 mN applied for 10 s.

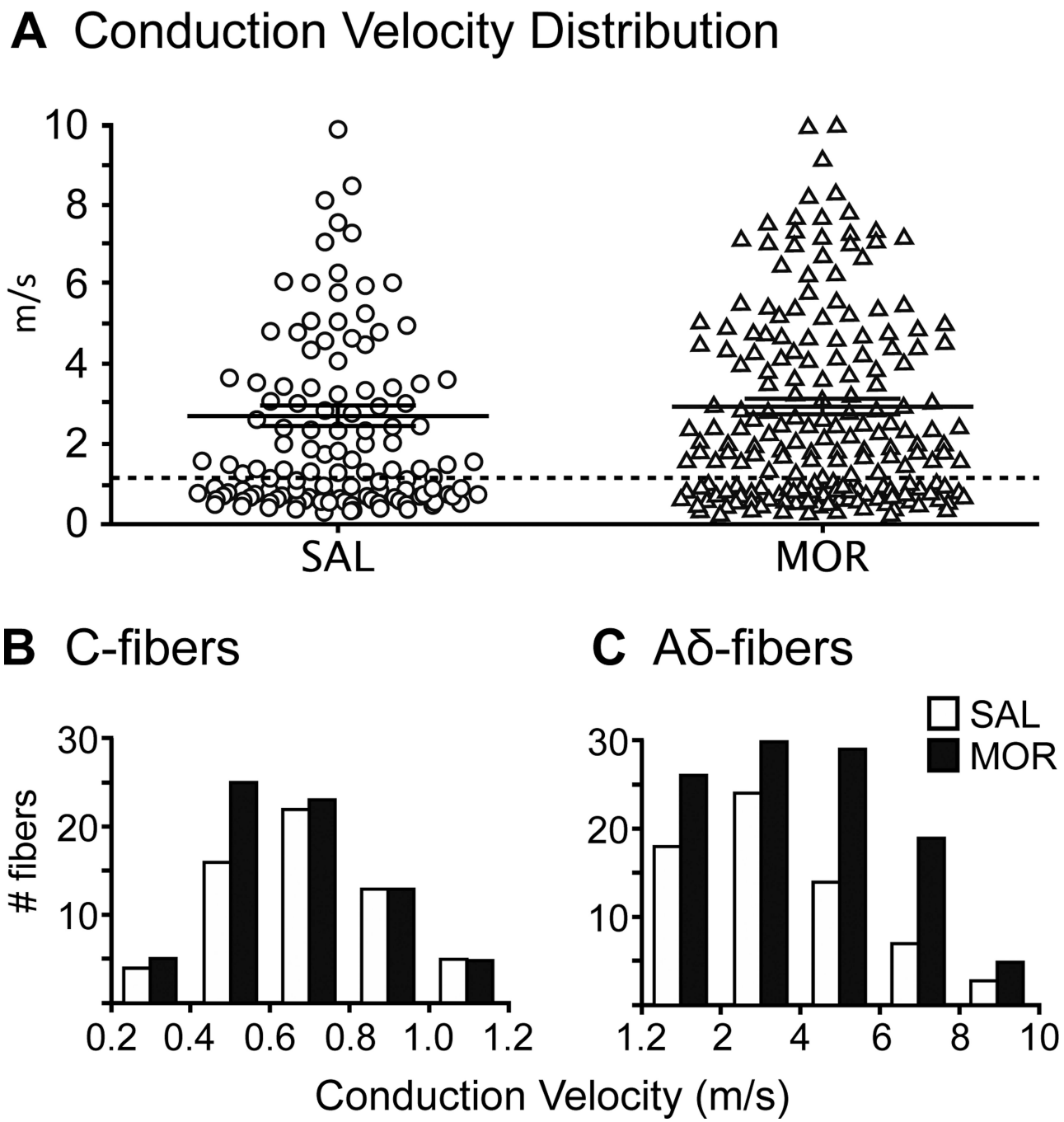

Figure 3.

Morphine treatment does not affect conduction velocity (CV) of nociceptors. A) Scatter plots of the CV of all fibers recorded in SAL and MOR mice (lines represent mean ± SEM). The mean CV's (SAL fibers = 2.7 ± 0.3 m/s, MOR fibers = 2.9 ± 0.2 m/s) were not significantly different (Mann Whitney test; $p > 0.05$). Morphine treatment does not change the distribution of CV of nociceptors (B,C). Conduction velocities of C- and Aδ-fibers were determined in naïve mice by measuring compound action potentials in the sciatic/tibial nerves (n = 3).

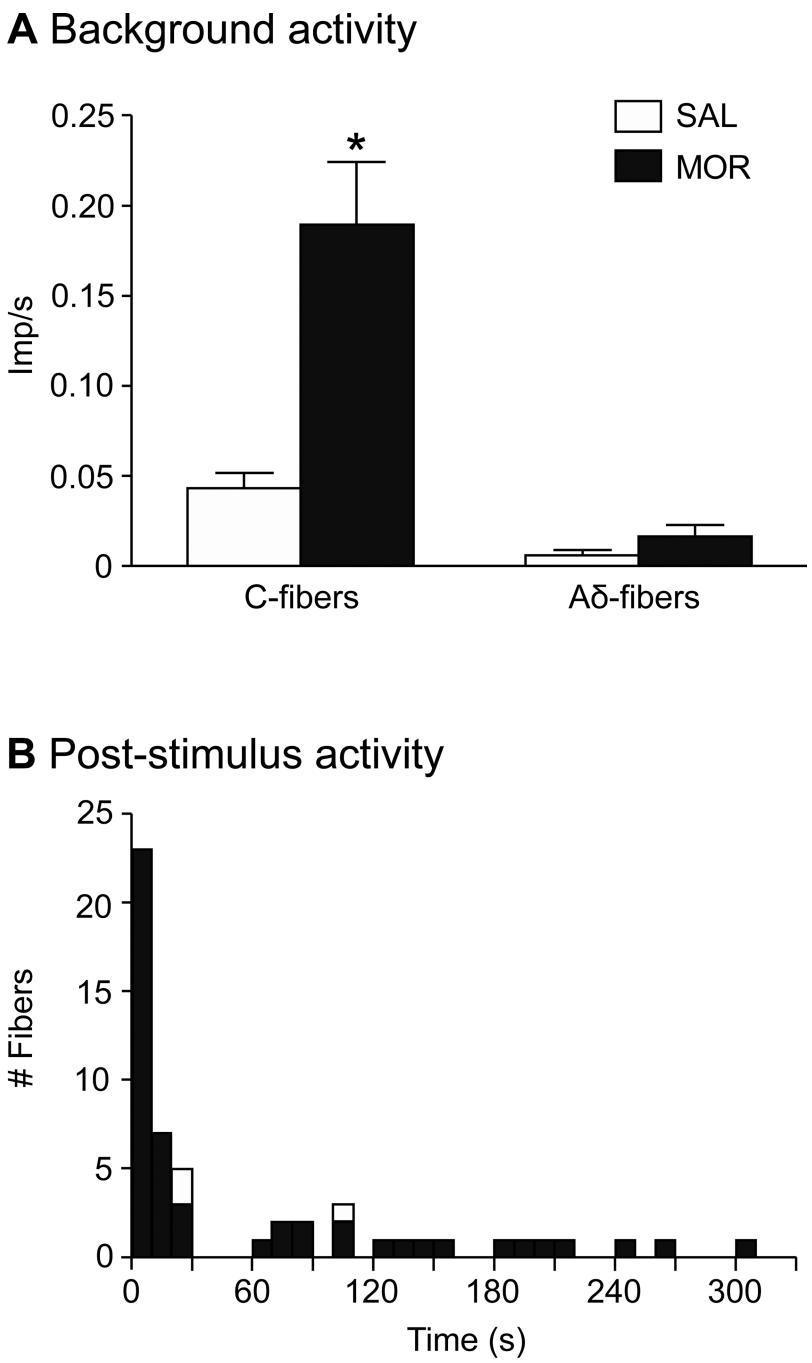

Figure 4.

Morphine treatment significantly increased resting background activity and afterdischarge. A) Prior to any stimulation, C- and Aδ-fiber activity was collected during the first 2 min of the recording session. The mean discharge rate for C-fibers from MOR mice was significantly higher compared to SAL mice (unpaired t-test with Welsh's correction for unequal variances; *$p < 0.001$). There was no difference in Aδ-fiber activity between groups. B) Afterdischarge: Activity that began within 30 s of the end of a stimulus was considered related to that stimulus and termed afterdischarge. This time frame was based on the fact that when post-stimulus activity did occur, it was often continuous with the evoked response and/or began within 30 s post-stimulus. Notably, there was a period of silence that

occurred between 30 – 60 s post-stimulus, further demarcating the afterdischarge from other spontaneous activity events. Open boxes representing aberrant activity in SAL mice sit on top of the bars for MOR mice.

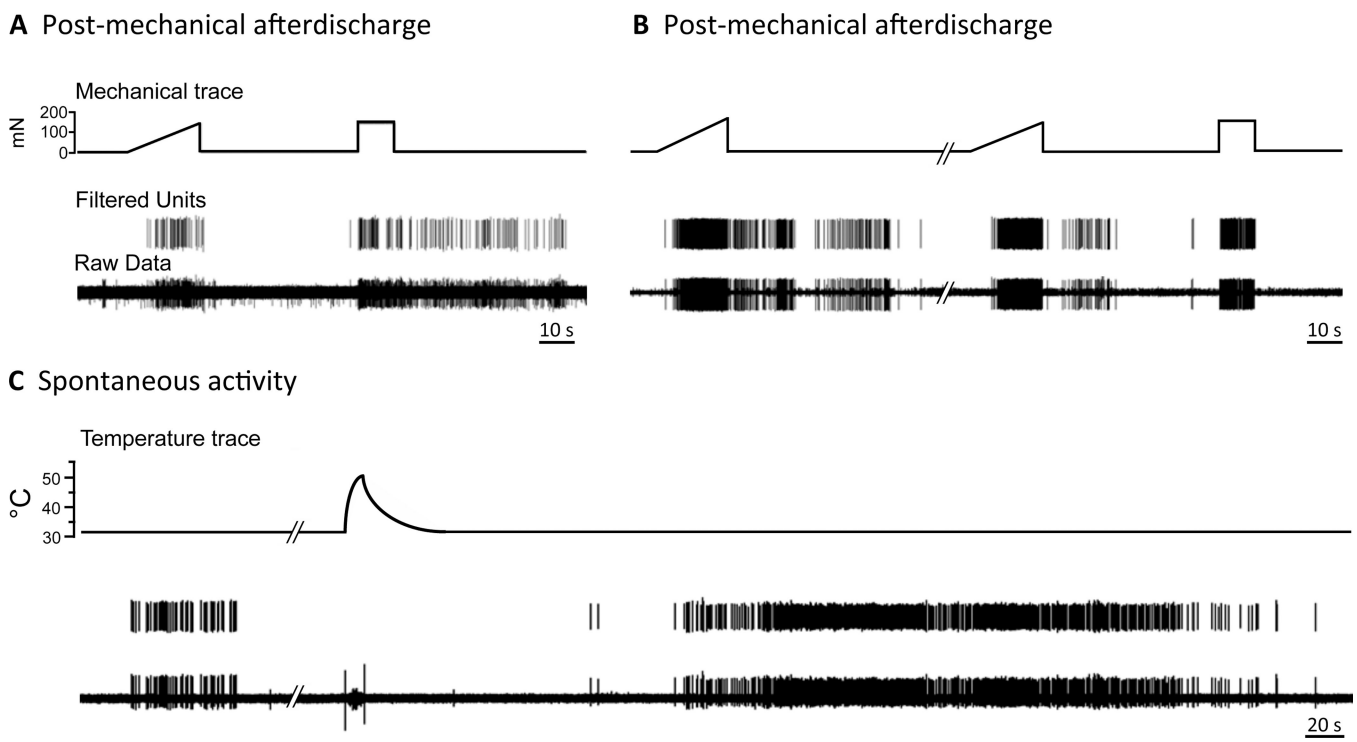

Figure 5.

Examples of aberrant activity patterns seen in fibers from MOR mice. A) Sustained afterdischarge following cessation of a stimulus. This CMC unit responds normally to the mechanical ramp stimulus, but it continues to discharge after the end of the square-wave mechanical pulse. B) Another example of afterdischarge. This AδMC unit responds normally to the square-wave mechanical pulse, but it continues to discharge after the end of two mechanical ramp stimuli. C) Un-evoked firing between stimuli. An AδM unit exhibits an event of spontaneous activity during the background recording interval. The unit displays another prolonged event of SA that is unrelated to the preceding heat stimulus.

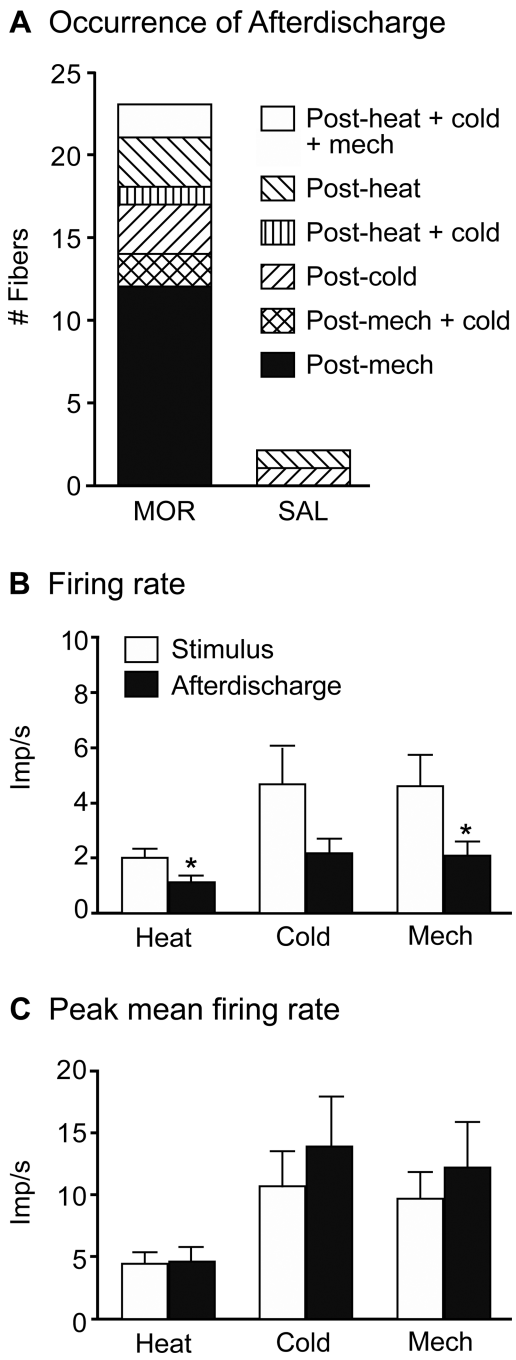

Figure 6.

Characteristics of afterdischarge in MOR mice. A) Fibers could demonstrate afterdischarge in relation to one or more stimulus modalities, i.e. following mechanical only (Post-mech) or following mechanical and cold (Post-mech + cold). B) The firing rate during afterdischarge, while robust, was significantly less than that occurring during the stimulus (one-way ANOVA; *$p < 0.05$). C) The peak firing rate during afterdischarge was equal to that occurring during stimulation.

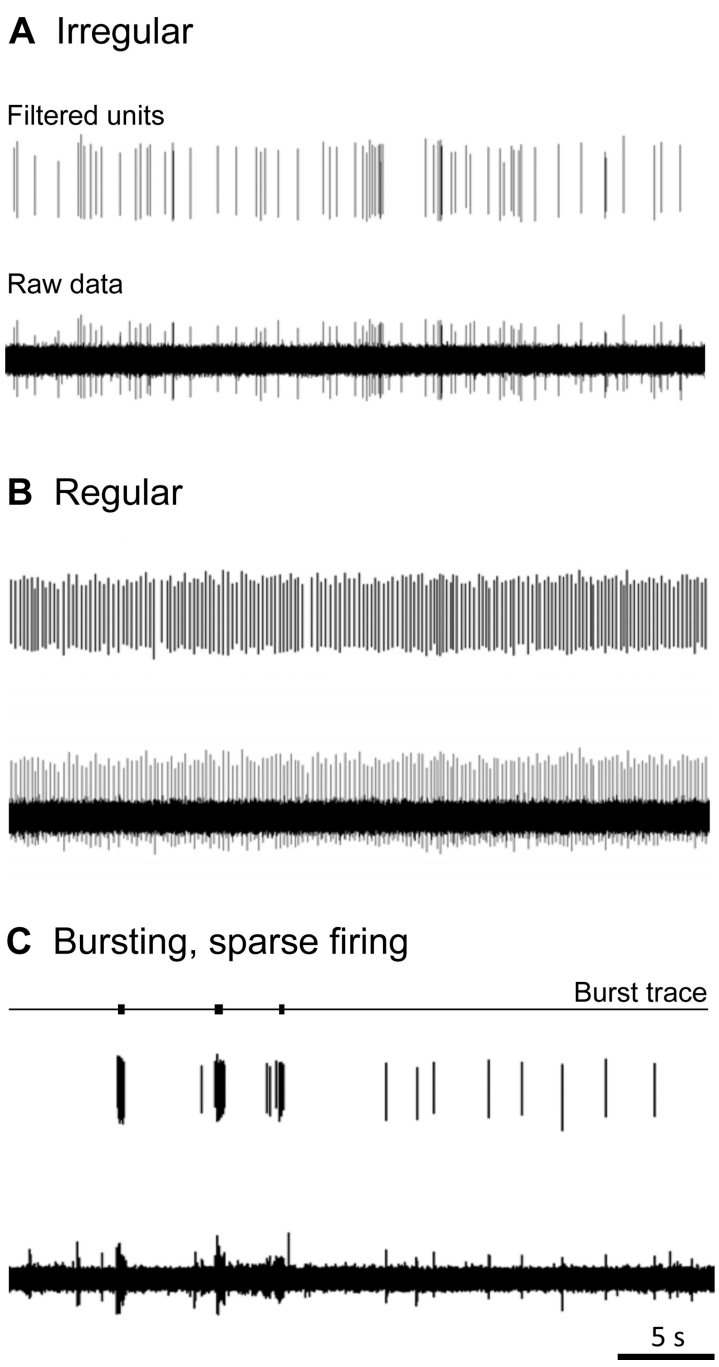

Figure 7.

Spontaneous activity in fibers from MOR mice was characterized as irregular, regular or bursting based on inter-spike interval histograms. A) Example of an irregular firing pattern with a firing rate of 1.7 imp/s. The top trace shows the filtered unit, the bottom trace shows the raw data. B) Example from an episode of regular firing. The top trace shows the filtered unit; the bottom trace shows the raw data. Overall the unit has a regular firing pattern with a mean rate of 3.9 imp/s. C) Predominately burst-like firing. Locations of burst activity as identified by Spike2 are marked by black rectangles in the top trace. The middle trace shows the filtered unit, the bottom trace shows the raw data. This unit shows sparse overall firing

(0.6 imp/s) with 84.4% of the spikes falling within bursts with an intraburst rate of 28.8 imp/s.

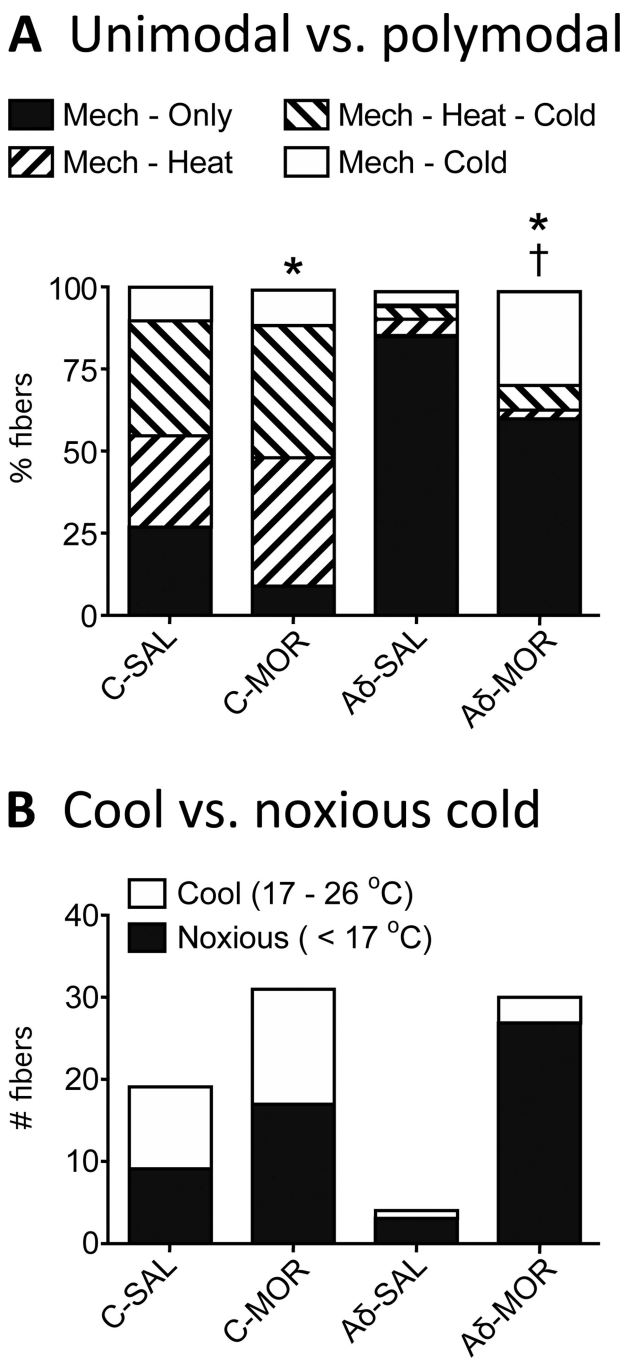

Figure 8.

A) Morphine treatment significantly decreases the number of unimodal fibers (mechanical only) in both the C (Fisher's exact test; *$p < 0.05$) and Aδ population (Fisher's exact test; *$p < 0.001$). For polymodal C-fibers, the CMH, CMHC and CMC populations expanded approximately equally. For Aδ-fibers, the increase in polymodal fibers was entirely due to an increase in AδMC-fibers (Fisher's exact test; $^{\dagger}p < 0.0001$, comparing MOR vs SAL). B) For C-fibers, there was a similar increase in units responding at cool vs cold temperature ranges. The increase in cold sensitive C-fibers was divided between those with thresholds in the moderate cooling range and the noxious cold range. For Aδ-fibers, the increase in cold

sensitive fibers was almost entirely in the population with thresholds in the noxious cold range (< 17°C).

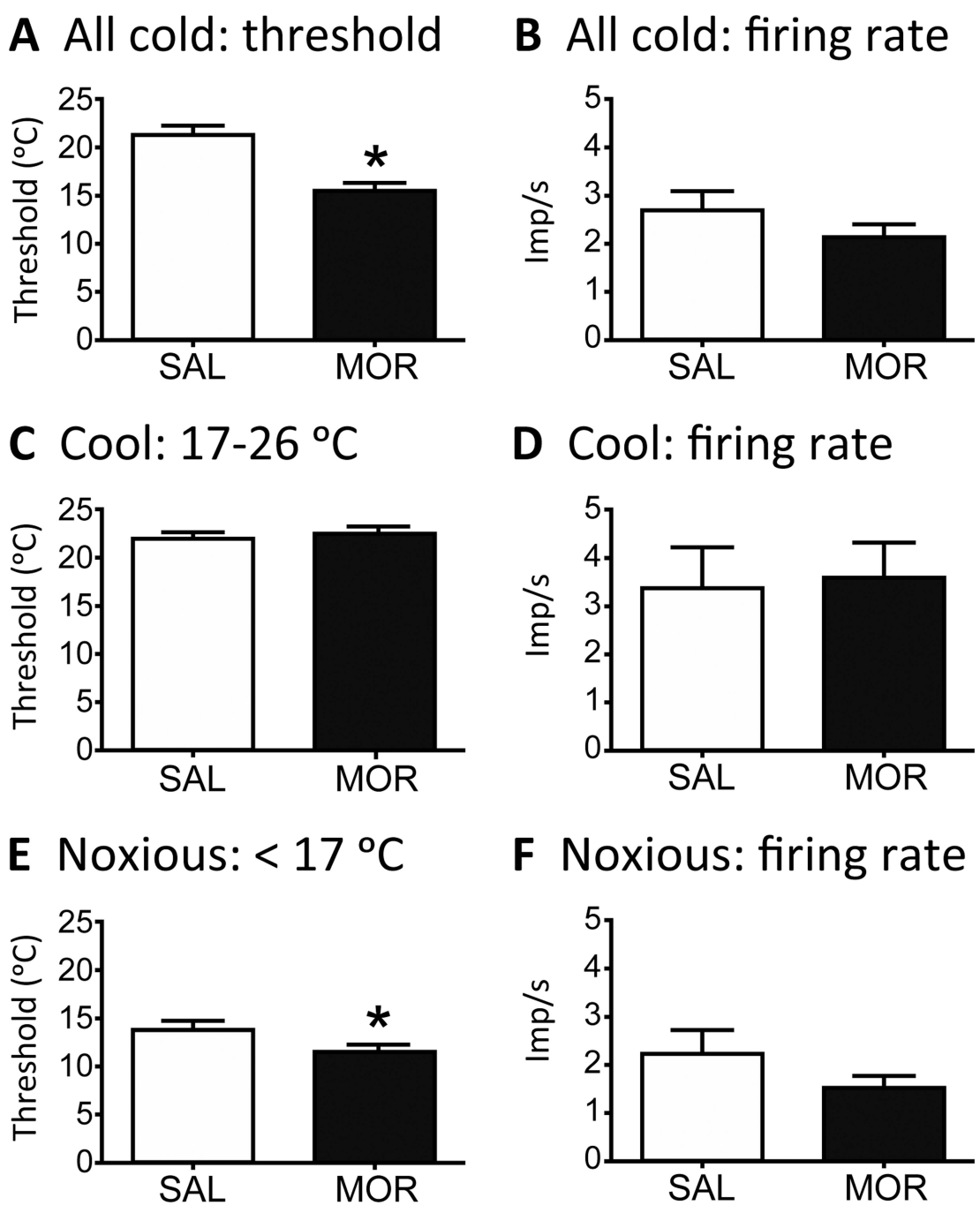

Figure 9.

Response characteristics of nociceptors to cold stimulation. Because few Aδ-fibers are normally sensitive to cold, C- and Aδ-fibers are pooled for this analysis. A) Fibers from MOR mice show a significantly colder threshold to activation compared to SAL mice (student's t-test; *$p < 0.001$). B) The firing rate of nociceptors to cold stimulation does not change in MOR mice. C–F) Units were further divided into those responding to moderate cooling (threshold between 26 and 17°C) and noxious cold (threshold < 17 °C). There was no difference between MOR and SAL mice in threshold (C) or firing rate (D) of fibers in the moderate cooling range. For noxious cold, the threshold was significantly lower (colder)

comparing MOR to SAL mice (E, student's t-test; *$p < 0.05$), but there was no change in the firing rate (F).

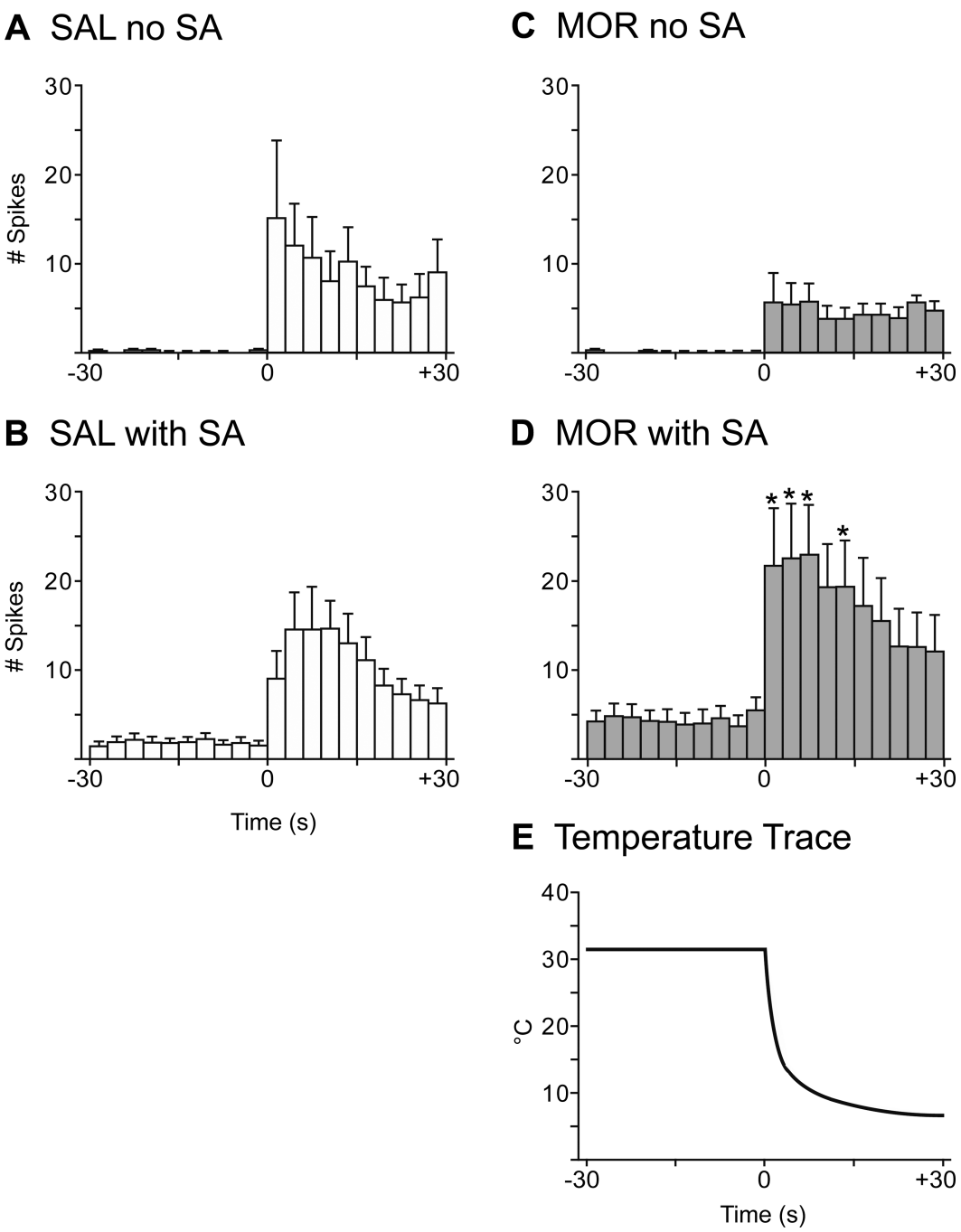

Figure 10.

Peristimulus histograms demonstrating temperature-dependent cold repsonses. Graphs show the number of spikes in 3 s bins. Units were separated into those with and without ongoing activity prior to cold stimulation. SAL units with (B, n = 11) or without (A, n =11) ongoing activity showed significant temperature-dependent cold responses as did MOR units with ongoing activity (D, n = 17). In contrast, MOR units without ongoing activity (C, n = 13) showed an increase in discharge rate, but the activity was not temperature-dependent. Cold stimulation produced firing rates that were significantly elevated from time 0–9 s and 12–15 s in MOR units with ongoing activity, compared to MOR units without ongoing activity. E) Typical trace showing the decrease in temperature once the SIF pellet was placed in the

well. (Two-way repeated measures ANOVA with post-hoc Bonferroni multiple comparisons; *$p < 0.05$.)

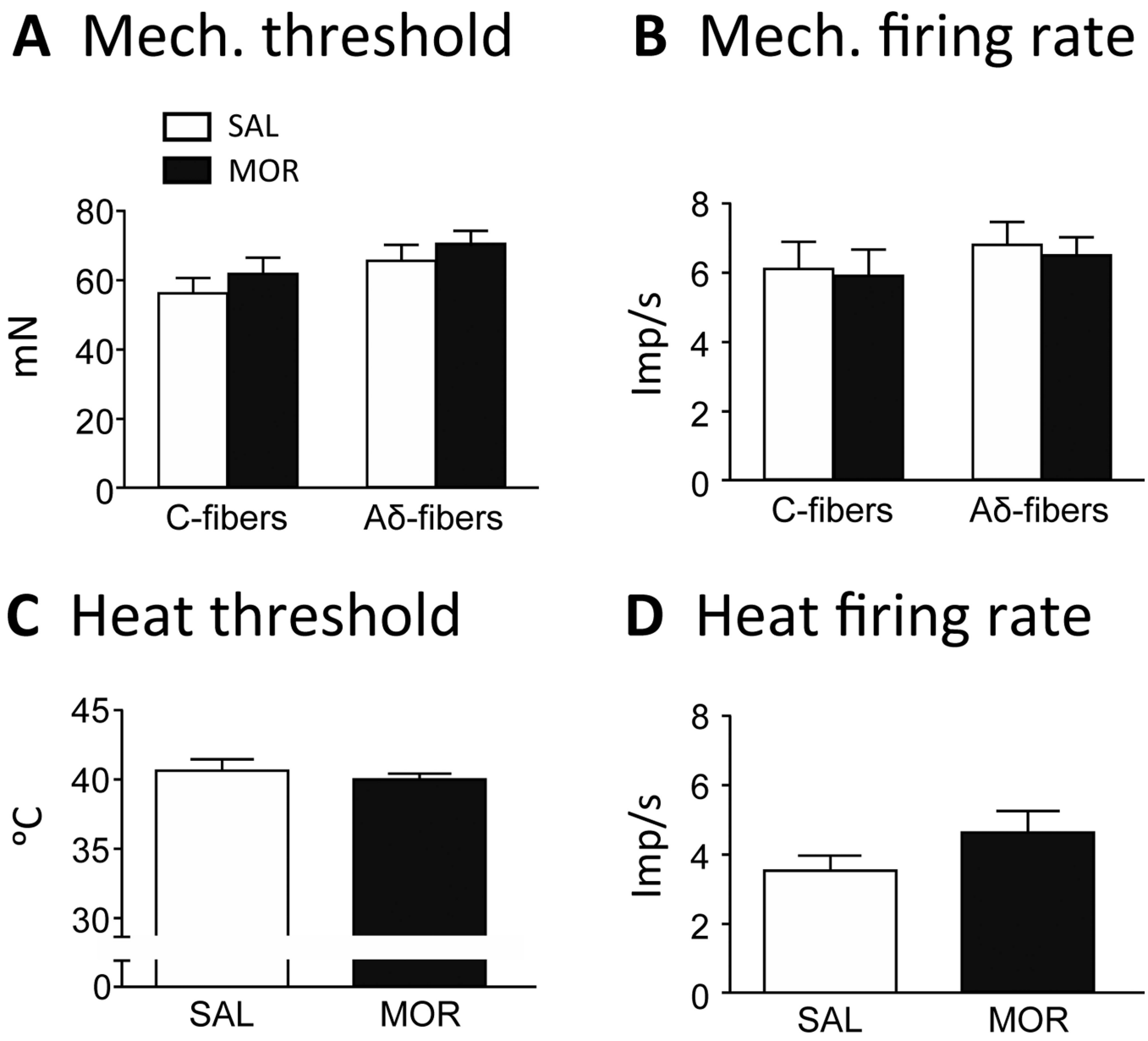

Figure 11.

Morphine treatment did not change response characteristics of nociceptors to mechanical or heat stimulation. Mechanical threshold (A) and firing rate (B) did not change significantly in C- or Aδ-fibers in MOR compared to SAL mice (one-way ANOVA; $p > 0.05$). Heat threshold (C) and firing rate (D) did not change significantly in C- or Aδ-fibers in MOR compared to SAL mice (t-test; $p > 0.05$).

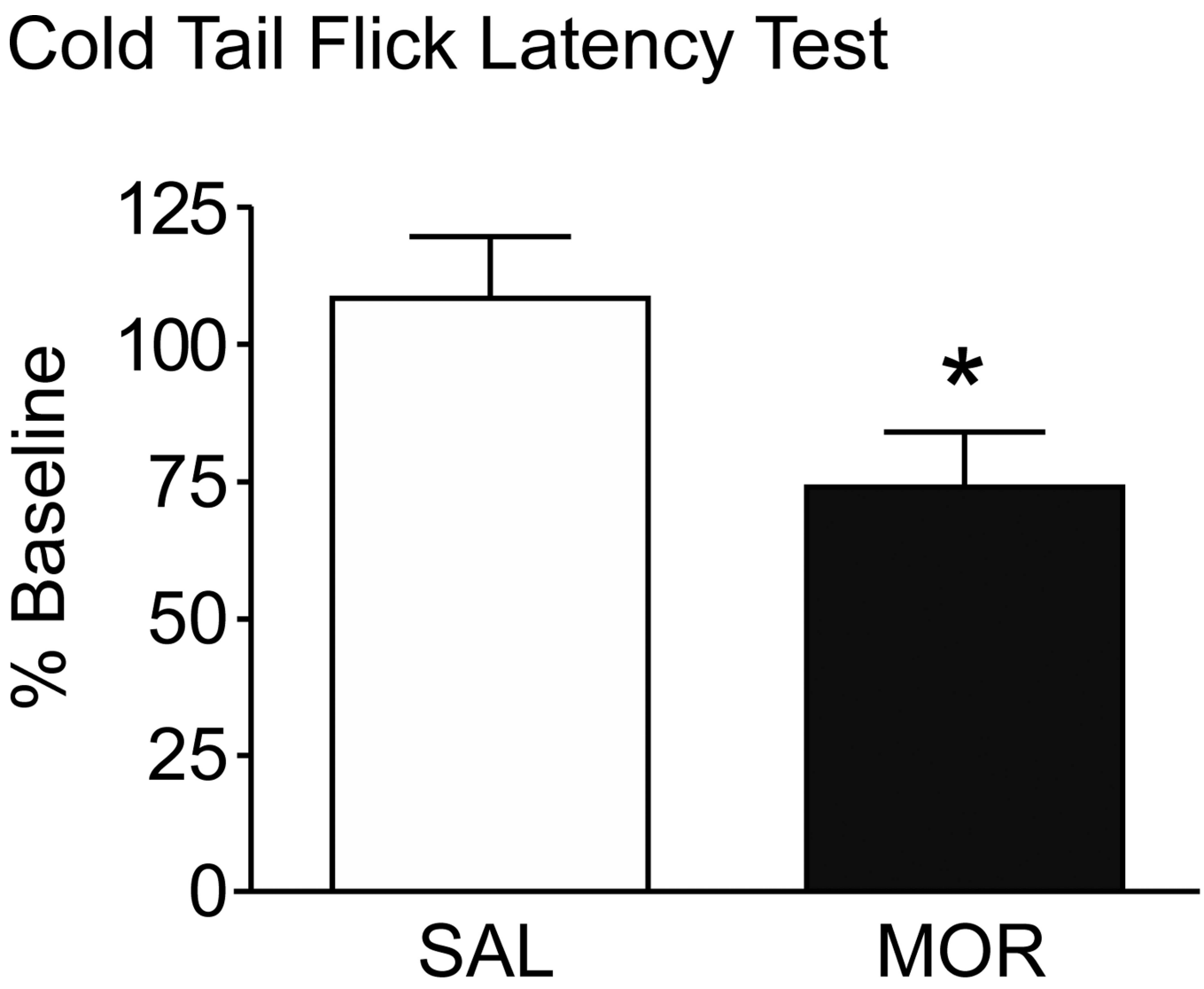

Figure 12.
Compared to SAL mice, MOR mice were more sensitive in the cold tail flick test, having a shorter latency to remove their tail from the cold water. Data are expressed as a percentage of baseline (t-test; *$p < 0.05$).

Table 1

Characteristics of fibers displaying afterdischarge and/or SA

	Fiber Type	Post-stimulus interval	Duration (s)	Firing rate (Imp/s)	Peak Mean Freq. (Imp/s)
Afterdischarge MOR	n = 23	6.5 ± 1.4 (0 – 24.2)	225.2 ± 33.1 (27.6 – 747.7)	1.9 ± 0.4 (0.2 – 4.3)	11.3 ± 2.5 (2.0 – 61.8)
Afterdischarge SAL	n = 2	25.2 ± 0.1 (25.1 – 25.3)	376.8 ± 143.0 (233.8 – 519.7)	0.8 ± 0.1 (0.7 – 0.9)	4.6 ± 0.8 (3.9 – 5.4)
SA MOR	n = 26	153.4 ± 16.8 (61.7 – 304.5)	129.0 ± 15.0 (28.1 – 412.9)	1.3 ± 0.2 (0.4 – 7.0)	7.8 ± 1.1 (2.0 – 19.0)
SA SAL	n = 1	109.3	194.8	0.7	4.9

Parameters of nociceptors displaying afterdischarge and SA expressed as average ± SEM, with the range of values in parenthesis. Post-stimulus interval represents that time when the stimulus stops and the unit starts to fire again. Duration is the length of the period of aberrant activity. Firing rate is the average rate for the whole event. Maximum mean frequency is the maximum firing rate reached during the event. Afterdischarge is defined as prolonged firing beginning within 30s after the end of a stimulus. Spontaneous activity includes those fibers showing episodes of firing not associated with a stimulus (post-stimulus interval is > 60 s). Some fibers showed more than one kind of activity.

Table 2

Characteristics of firing patterns of nociceptive fibers

	Pattern	Duration (s)	Firing rate (Imp/s)	Max. Mean Freq. (Imp/s)	% Spikes in Bursts
MOR	Irregular (n=27)	149.4 ± 16.2 (24.1 – 412.9)	0.9 ± 0.07 (0.2 – 2.2)	5.3 ± 0.5 (2.0 – 13.5)	1.3% ± 0.8 (0 – 11.8)
	Regular (n=11)	296.6 ± 53.2 (27.6 – 747.7)	2.3 ± 0.3 (0.5 – 4.3)	9.8 ± 2.5 (3.0 – 40.2)	7.6% ± 3.0 (0 – 38.1)
	Bursting (n=9)	84.7 ± 13.0 (19.9 – 145.4)	3.3 ± 0.9 (0.6 – 10.4)	23.0 ± 4.5 (11.2 – 61.8)	72.4% ± 5.4 (40.0 – 92.0)
SAL	Irregular (n=3)	316.1 ± 102.4 (194.8 – 519.7)	0.7 ± 0.06 (0.7 – 0.9)	4.7 ± 0.5 (3.9 – 5.4)	0

Parameters of irregular, regular and burst firing expressed as average ± SEM, with the range of values in parenthesis. Duration is the length of the period of aberrant activity. Firing rate is the average rate for the whole event. Maximum mean frequency is the maximum firing rate reached during the event. Percentage of spike in bursts shows the percentage of spikes from the total event that occur within bursts rather than between bursts.

Table 3

Population of nociceptive fibers recorded in the plantar nerve

Unit Type	C-SAL	C-MOR	p value	Aδ-SAL	Aδ-MOR	p value
Unimodal	26.7% (16)	9.7% (7)	***0.01**	86.4% (57)	60.3% (70)	***0.0002**
Mech - Heat	28.3% (17)	38.9% (28)	0.27	4.5% (3)	2.6% (3)	0.67
Mech - Heat - Cold	35.0% (21)	40.3% (29)	0.54	4.5% (3)	7.8% (9)	0.54
Mech - Cold	10.0% (6)	11.1% (8)	1.00	4.5% (4)	29.3% (34)	***<0.0001**

Due to our search stimulus, all nociceptive fibers are mechanically sensitive. Values are percentages with numbers of fibers in parentheses. SAL mice are compared to MOR mice using Fisher's exact test; $p < 0.05$ is considered significant.